Subduction initiation in the Scotia Sea region and opening of the Drake Passage: When and why?

Review Article

Author(s):
van de Lagemaat, Suzanna H.A.; Swart, Merel L.A.; Vaes, Bram; Kosters, Martha E.; Boschman, Lydian (iD); Burton-Johnson, Alex; Bijl, Peter K.; Spakman, Wim; van Hinsbergen, Douwe J.J.

Subduction initiation in the Scotia Sea region and opening of the Drake Passage: When and why?

Suzanna H.A. van de Lagemaat [a],[*], Merel L.A. Swart [a], Bram Vaes [a], Martha E. Kosters [a], Lydian M. Boschman [a],[b], Alex Burton-Johnson [c], Peter K. Bijl [a], Wim Spakman [a], Douwe J. J. van Hinsbergen [a]

[a] Department of Earth Sciences, Utrecht University, Princetonlaan 8A, 3584 CB Utrecht, the Netherlands
[b] Department of Environmental System Science, ETH Zürich, Universitätstrasse 16, 8092 Zürich, Switzerland
[c] British Antarctic Survey, High Cross, Madingley Road, Cambridge CB3 0ET, United Kingdom

A B S T R A C T

During evolution of the South Sandwich subduction zone, which has consumed South American Plate oceanic lithosphere, somehow continental crust of both the South American and Antarctic plates have become incorporated into its upper plate. Continental fragments of both plates are currently separated by small oceanic basins in the upper plate above the South Sandwich subduction zone, in the Scotia Sea region, but how fragments of both continents became incorporated in the same upper plate remains enigmatic. Here we present an updated kinematic reconstruction of the Scotia Sea region using the latest published marine magnetic anomaly constraints, and place this in a South America-Africa-Antarctica plate circuit in which we take intracontinental deformation into account. We show that a change in marine magnetic anomaly orientation in the Weddell Sea requires that previously inferred initiation of subduction of South American oceanic crust of the northern Weddell Sea below the eastern margin of South Orkney Islands continental crust, then still attached to the Antarctic Peninsula, already occurred around 80 Ma. Subsequently, between ~71–50 Ma, we propose that the trench propagated northwards into South America by delamination of South American lithosphere: this resulted in the transfer of delaminated South American continental crust to the overriding plate of the South Sandwich subduction zone. We show that continental delamination may have been facilitated by absolute southward motion of South America that was resisted by South Sandwich slab dragging. Pre-drift extension preceding the oceanic Scotia Sea basins led around 50 Ma to opening of the Drake Passage, preconditioning the southern ocean for the Antarctic Circumpolar Current. This 50 Ma extension was concurrent with a strong change in absolute plate motion of the South American Plate that changed from S to WNW, leading to upper plate retreat relative to the more or less mantle stationary South Sandwich Trench that did not partake in the absolute plate motion change. While subduction continued, this mantle-stationary trench setting lasted until ~30 Ma, after which rollback started to contribute to back-arc extension. We find that roll-back and upper plate retreat have contributed more or less equally to the total amount of ~2000 km of extension accommodated in the Scotia Sea basins. We highlight that viewing tectonic motions in a context of absolute plate motion is key for identifying slab motion (e.g., rollback, trench-parallel slab dragging) and consequently mantle-forcing of geological processes.

1. Introduction

Subduction zones form during plate motion reorganizations, either by breaking a single plate into two independently moving plates, or by inverting a transform or ridge (e.g., Auzemery et al., 2020; Gurnis et al., 2004; Maffione et al., 2015; Stern, 2004). Interestingly, in the case of the South Sandwich subduction zone, which now forms an isolated trench in the South Atlantic Ocean, it is difficult to assess which of these mechanisms played a role. The overriding plate, to the west of the South Sandwich subduction zone, contains continental fragments that rifted

from both the Antarctic Peninsula, part of the Antarctic Plate, as well as from Tierra del Fuego (southern Patagonia), part of the South American Plate. These continental fragments are currently separated by small oceanic basins (Civile et al., 2012; Dalziel et al., 2013; Eagles and Livermore, 2002; Vuan et al., 2005). Interestingly, continental blocks derived from both the Antarctic and the South American Plate were part of the same upper plate, above the South Sandwich subduction zone. Since its formation, this subduction zone has been consuming South American oceanic lithosphere that formed the conjugate of the lithosphere underlying the Weddell Sea, which is part of the Antarctic Plate. Explaining the presence of Antarctica-derived lithospheric fragments in the upper plate of the South Sandwich subduction zone thus merely requires finding when the South American and Antarctic plates may have converged in the Drake Passage region (Figs. 1 and 2). Different scenarios have been proposed to explain this (Barker, 2001; Dalziel et al., 2013; Eagles, 2016b; Lagabrielle et al., 2009; Vérard et al., 2012). What remains puzzling is that South American Plate fragments also ended up in the upper plate of the South Sandwich subduction zone.

In the search for causes of subduction initiation, previous studies have looked for evidence for convergence in the Drake Passage region. Two causes for subduction initiation have been proposed. The first is that westward motion of Tierra del Fuego relative to the Antarctic Peninsula led to the development of an active margin to the east of South Orkney Islands continental crust, then still part of the Antarctic Peninsula, and the westward subduction of oceanic crust of the South American Plate (Barker, 2001; Eagles and Jokat, 2014; Lagabrielle et al., 2009; Vérard et al., 2012). The proposed timing of this event varies from latest Cretaceous (~70 Ma; Vérard et al., 2012) to Eocene (~46 Ma; Lagabrielle et al., 2009; ~50 Ma; Eagles and Jokat, 2014). This does not explain, however, how South American oceanic lithosphere subduction below the Tierra del Fuego region began. The second hypothesis is that such subduction within South America may somehow be linked to the mid-Cretaceous closure of the South American Rocas Verdes Basin (Barker, 2001; Dalziel et al., 2013), unrelated to subduction below the Antarctic Peninsula.

The aim of this study is to develop a geodynamic scenario for the origin and evolution of the Scotia Sea that addresses: 1) when and why a subduction zone first formed between South America and the Antarctic Peninsula and 2) when and why this subduction zone may have propagated, or initiated, into the South American Plate, and how South American continental lithosphere transferred to the upper plate of the South Sandwich subduction zone. To this end, we have developed a kinematic restoration back to the time of Gondwana break-up embedded in a global plate reconstruction framework. We use a plate circuit through Africa, by restoring the opening of the South Atlantic and Southwest Indian oceans based on previously published marine geophysical constraints. We first restore the extensional history of the Scotia Sea recorded by the small oceanic basins using published marine magnetic anomaly data. Then, to assess the amount of pre-drift extension (i.e., the continental rifting phase before oceanic spreading), we use the plate circuit and published marine magnetic anomalies in the Weddell Sea ocean floor to approximate the location of the South American ocean-continent transition to the Weddell Sea conjugate ocean floor. To assess the Antarctic Peninsula-Patagonia convergence in driving subduction initiation, we also correct for intracontinental deformation within South America and Antarctica and test this against a new compilation of paleomagnetic data. Based on our reconstruction, which we study in both relative and absolute plate motion context, we propose a new view on the timing and geodynamic forcing for the initiation and evolution of subduction, its propagation into the South American Plate, the transition to upper plate extension in the Scotia Sea region, and its subsequent evolution that led to opening of the Drake Passage.

2. Modern geological architecture of the Scotia Sea region

The Scotia Sea is underlain by the Scotia and South Sandwich plates (Fig. 1). Major tectonic plates that surround both plates are the South American Plate in the north and east and the Antarctic Plate in the south and west (Figs. 1, 2 and 3). To the southeast of the South Sandwich subduction zone, there is a short segment of the South American-Antarctica plate boundary that ends in a triple junction with the South
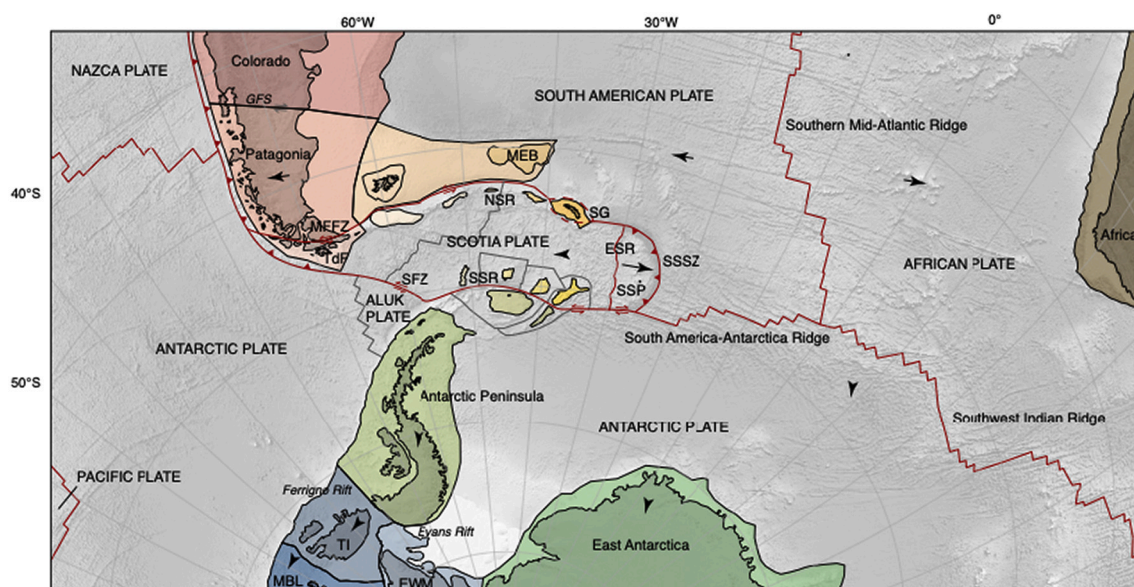
Fig. 1. Tectonic map of the Scotia Sea Region. The map shows the main faults, plate boundaries and tectonic blocks (colored polygons) discussed in this paper. Major plates are given in capital letters. Active plate boundaries are indicated with red lines. The plate boundary around South Georgia is dashed, as it is being transferred from the north to the south of the microcontinent (Smalley Jr. et al., 2019). Former plate boundaries of the Scotia Sea region in gray. Coastlines of West Antarctica tectonic blocks are based on present-day continental lithosphere that rises above sea-level. Black arrows represent plate motions relative to the mantle in the last 5 Myr in the reference frame of Doubrovine et al. (2012). Abbreviations: ESR = East Scotia Ridge; EWM = Ellsworth – Whitmore Mountains; GFZ = Gastre Fault Zone; MBL = Marie Byrd Land; MFFZ = Magallanes-Fagnano Fault Zone; MEB = Maurice Ewing Bank; NSR = North Scotia Ridge; SG = South Georgia; SSP = South Sandwich Plate; SSR = South Scotia Ridge; SSSZ = South Sandwich subduction zone; TdF = Tierra del Fuego; TI = Thurston Island.
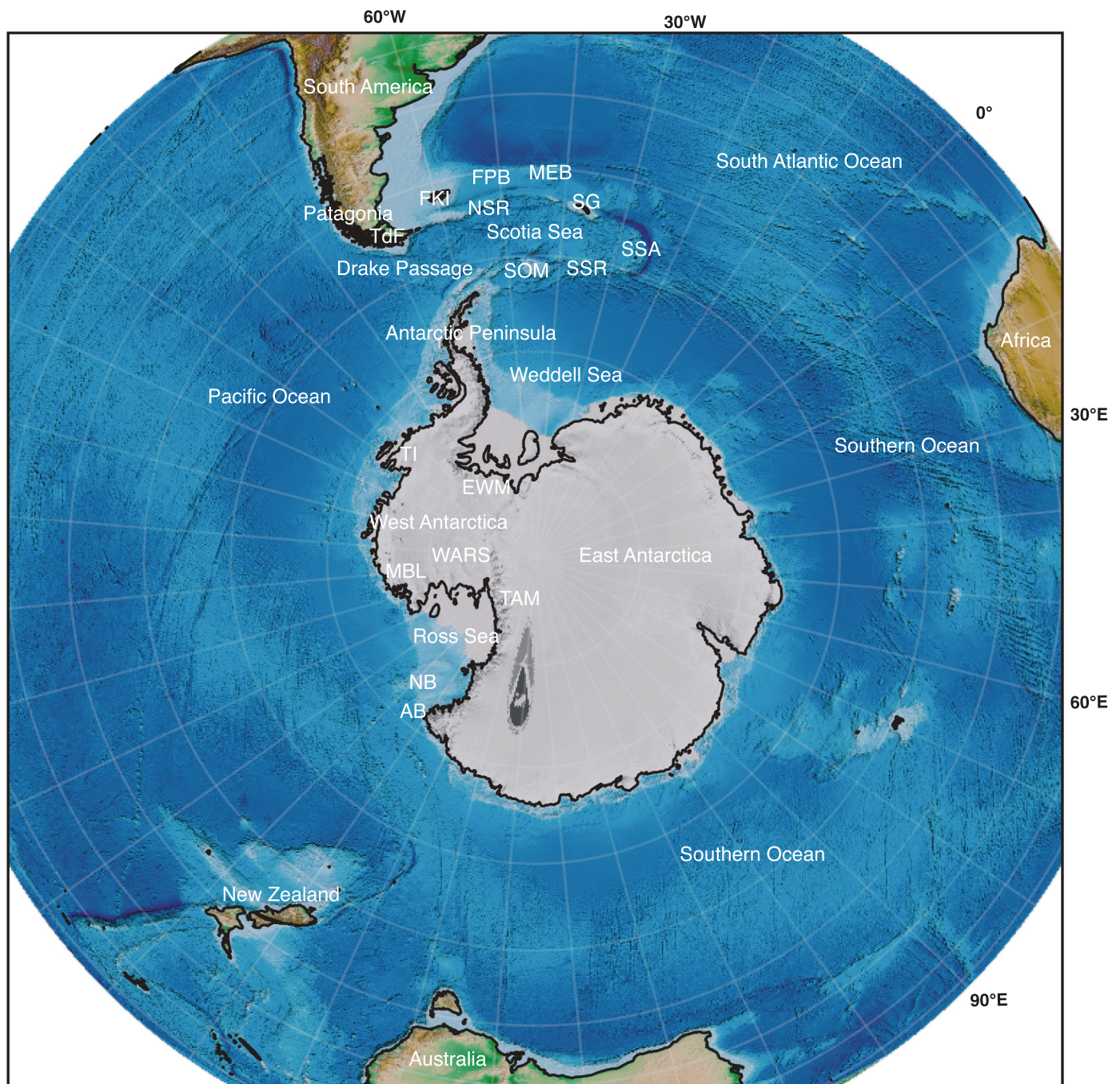
Fig. 2. Geographic map of the Circum-Antarctic region. Abbreviations: AB = Adare Basin; EWM = Ellsworth-Whitmore Mountains; FKI = Falkland Islands; FPB = Falkland Plateau Basin; MEB = Maurice Ewing Bank; MBL = Marie Byrd Land; NB = Northern Basin; NSR = North Scotia Ridge; TdF = Tierra del Fuego; TI = Thurston Island; SG = South Georgia; SOM = South Orkney Microcontinent; SSR = South Scotia Ridge; WARS = West Antarctic Rift System.

America-Africa and Africa-Antarctica spreading ridges (Fig. 1; Barker and Lawver, 1988; DeMets et al., 2010). In the Pacific Ocean to the west-northwest of the Scotia Sea, the South American and Antarctic plates are converging, which leads to the subduction of oceanic lithosphere of the Antarctic Plate below southern South America (Fig. 1).

The Scotia Plate is separated from the South Sandwich Plate in the east by an active spreading ridge; from South America in the north by the left-lateral Magallanes-Fagnano and North Scotia Ridge transform system; from the small remnant of the Aluk (or Phoenix, or Drake) Plate in the west by the sinistral Shackleton fracture zone; and from Antarctica in the south by a diffuse plate boundary characterised by distributed left-lateral transpression (Fig. 1) (Thomas et al., 2003). The South Sandwich

Plate is separated from the South American Plate in the east by the South Sandwich trench, and from Antarctica in the south by a diffuse, dextral transform plate boundary (Thomas et al., 2003).

The Scotia Plate hosts three main oceanic basins characterised by different magnetic anomaly orientations: The East, Central, and West Scotia basins (Figs. 3 and 4). Microcontinents, arc remnants, and intervening small oceanic basins to the south of the main Scotia Sea basins collectively form the South Scotia Ridge. These comprise, from east to west: 1) the Discovery Bank, separated by the Scan Basin from 2) the Bruce Bank, separated by the Dove Basin from 3) the Pirie Bank, separated by the Protector Basin from 4) the Terror Rise (Figs. 3 and 4). The southernmost part of the Scotia Sea, along the diffuse plate
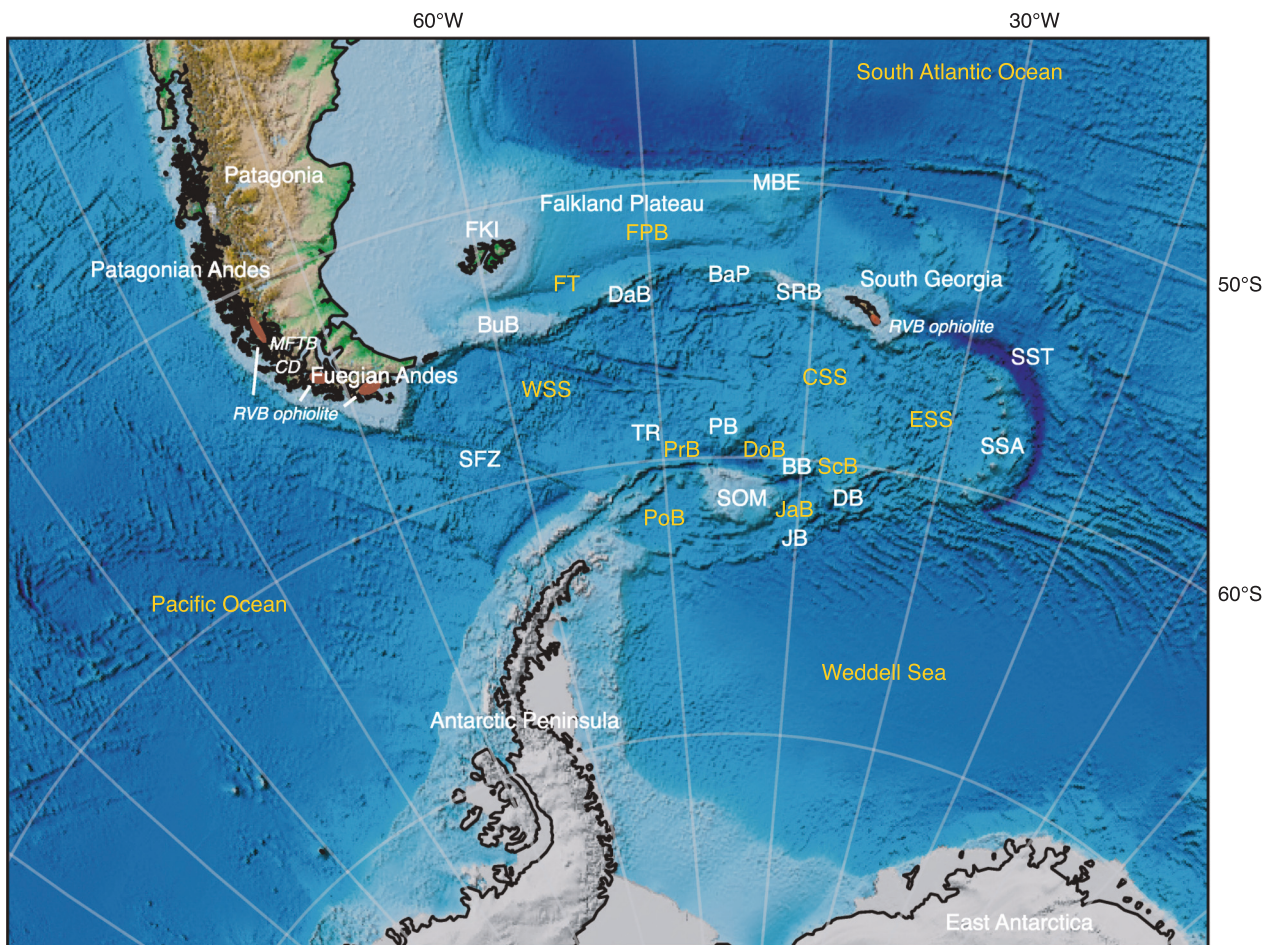
Fig. 3. Geographic map of the Scotia Sea region. Basin names in yellow, abbreviations: CSS = Central Scotia Sea; DoB = Dove Basin; ESS = East Scotia Sea; FT = Falkland Trough; FPB = Falkland Plateau Basin; JaB = Jane Basin; PoB = Powell Basin; PrB = Protector Basin; ScB = Scan Basin; WSS = West Scotia Sea. Other names in white, abbreviations: BaP = Barker Plateau; BB = Bruce Bank; BuB = Burdwood Bank; CD = Cordillera Darwin; DaB = Davis Bank; DB = Discovery Bank; JB = Jane Bank; FKI = Falkland Islands; MBE = Maurice Ewing Bank; MFTB = Magallanes Fold-and-Thrust-Belt; PB = Pirie Bank; RVB = Rocas Verdes Basin; SFZ = Shackleton Fracture Zone; SRB = Shag Rocks Bank; SSA = South Sandwich Arc; SST = South Sandwich Trench; TR = Terror Rise.

boundary with Antarctica, hosts from east to west the Jane Bank separated by the Jane Basin from the South Orkney microcontinent, separated by the Powell Basin from the Antarctic Peninsula (Fig. 3). Based on seismic data and dredge samples, Terror Rise and the Bruce and Pirie banks are considered to be underlain by extended continental crust (Eagles et al., 2006; Lodolo et al., 2010; Udintsev et al., 2012; Vuan et al., 2005). Dredging of the Discovery and Jane Banks have returned samples with a continental affinity (Lodolo et al., 2010), as well as arc-type magmatic rocks of unknown age (Barker et al., 1984; Barker et al., 1982). The geology of South Orkney Islands shows that they consist of continental crust that likely formed in Paleozoic time by accretion at the Panthalassa margin (Matthews and Maling, 1967; Tanner et al., 1982). East of the Antarctic Peninsula and south of the South Scotia Ridge lies the Weddell Sea, with an ocean floor that is part of the Antarctic Plate (Figs. 1, 2 and 3).

The northern margin of the Scotia Plate is referred to as the North Scotia Ridge, comprising the Burdwood and Davis banks, Barker (previously named Aurora) Plateau, and Shag Rocks Bank, as well as the South Georgia microcontinent (Figs. 3 and 4). Based on field investigations of South Georgia, and geochemistry and geochronology of dredge samples of the North Scotia Ridge banks, they are interpreted as continental fragments that share a geological affinity with the Fuegian Andes (Carter et al., 2014; Dalziel et al., 1975; Mukasa and Dalziel, 1996; Pandey et al., 2010; Riley et al., 2019; Storey and Mair, 1982; Storey et al., 1977). The ridge is separated from the Falkland Plateau to

the north by the Falkland Trough, a bathymetric depression that formed as part of the South American-Scotia transform plate boundary (Figs. 1 and 3).

The Falkland Plateau, located east of Patagonia in the South Atlantic Ocean (Fig. 2), forms a large promontory of extended South American crust (Ewing et al., 1971; Tankard et al., 2012). The Falkland Islands and Maurice Ewing Bank are emergent portions of the Falkland Plateau, underlain by continental crust (Schimschal and Jokat, 2019). They are separated from each other by the oceanic Falkland Plateau Basin (Schimschal and Jokat, 2018).

The transition from the N-S trending Patagonian Andes to the E-W trending Fuegian Andes and Falkland Plateau (Fig. 3) is known as the Patagonian Orocline (Carey, 1955). This region consists of five main geological provinces. From west to east, these are: 1) an Upper Jurassic – Miocene magmatic arc (Patagonian Batholith) related to (paleo-)Pacific subduction (Guillot, 2016; Herve et al., 2007; Hervé et al., 1984; Pankhurst et al., 2000); 2) thrusted and uplifted, uppermost Jurassic to lowermost Cretaceous ocean floor volcanics and Lower Cretaceous volcaniclastics (Relics of the former Rocas Verdes Basin) (Cunningham, 1994; Dalziel et al., 1974; Olivero and Malumián, 2008; Stern and De Wit, 2003); 3) a metamorphic complex of Late Paleozoic basement rocks affected by Late Cretaceous – Cenozoic thick-skinned tectonics (Cordillera Darwin) (Cunningham, 1995; Klepeis et al., 2010; Klepeis, 1994b; Maloney et al., 2011); 4) the thin-skinned Magallanes fold-and-thrust belt, containing thrust sheets that incorporate Lower Cretaceous to
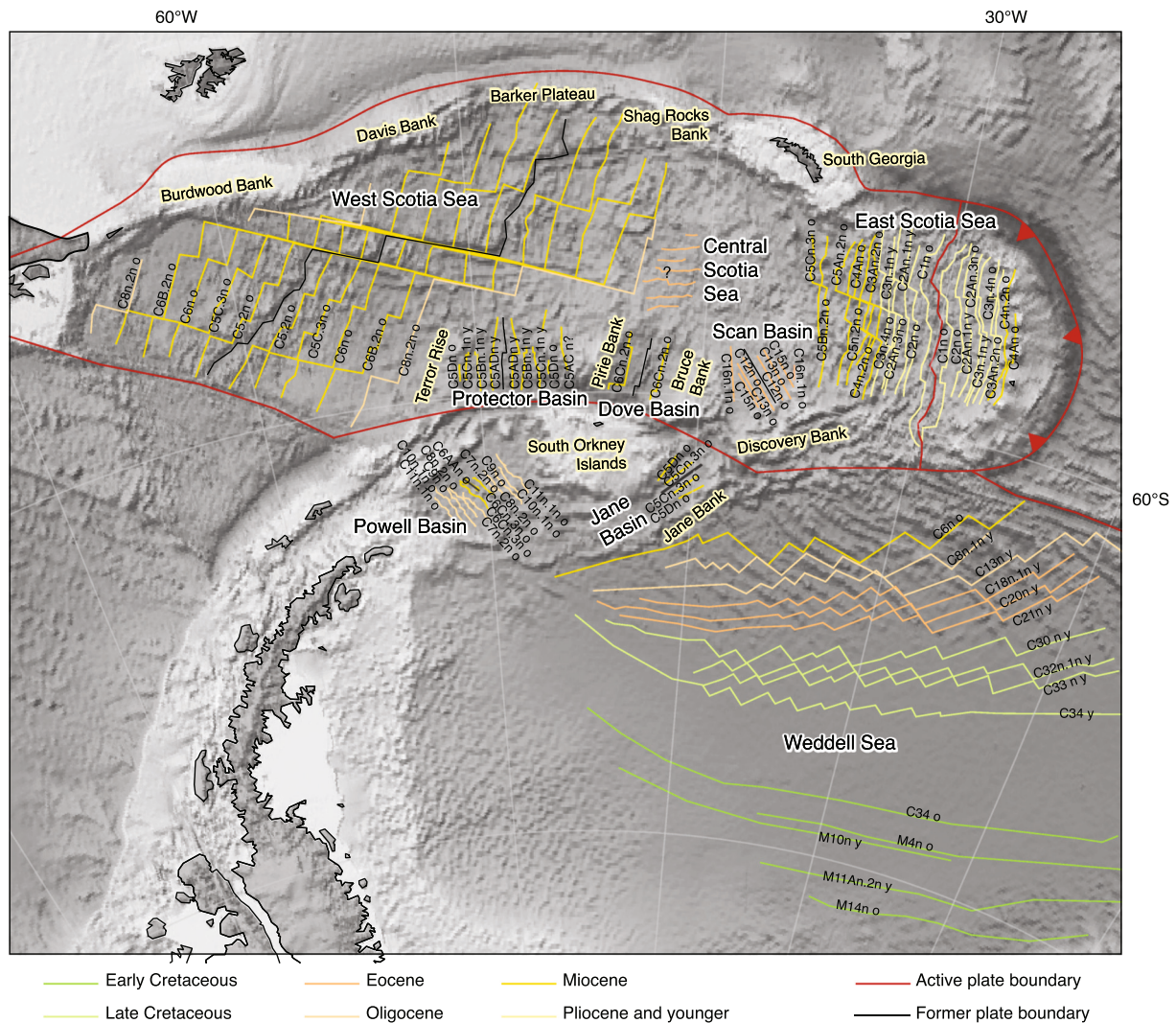
Fig. 4. Marine magnetic anomaly lineations map of the Scotia and Weddell Seas. Isochrons are labeled with chron interpretations and colored based on ages. References to anomaly identifications are given in Section 4.1.

Miocene continental and marine sequences of the Rocas Verdes back-arc and Austral foreland basin (Alvarez-Marrón et al., 1993; Betka et al., 2015; Betka, 2013; Ghiglione and Ramos, 2005; Ghiglione et al., 2009; Torres-Carbonell et al., 2013; Torres-Carbonell et al., 2017); and 5) an undeformed foreland (Austral and Magallanes basins) (Biddle et al., 1986; Ghiglione et al., 2010; Torres-Carbonell and Olivero, 2012). The southernmost Andes are cut by the Magallanes-Fagnano fault system, a left-lateral strike-slip fault system that marks the present-day onshore boundary between the Scotia and South American plates (Cunningham, 1993; Klepeis, 1994a; Pelayo and Wiens, 1989; Smalley Jr. et al., 2007; Smalley Jr. et al., 2003).

Antarctica is characterised by two different crustal realms, separated by the Transantarctic Mountains (Goodge, 2020) (Fig. 2). East Antarctica, facing the Atlantic and Indian Oceans, is a craton that formed during Precambrian and Cambrian times (Fitzsimons, 2000; Harley, 2003; Tingey, 1991). West Antarctica, facing the Pacific Ocean, comprises continental and arc crust of early Paleozoic age, divided into four major crustal blocks divided by fault or rift zones (Dalziel and Elliot, 1982; Gohl et al., 2007; Holt et al., 2006; Jordan et al., 2010): Thurston Island, Marie Byrd Land, Ellsworth-Whitmore Mountains, and the Antarctic Peninsula (Figs. 1 and 2; Dalziel and Elliot, 1982). Deformation within West Antarctica formed intracontinental basins and transform zones, most prominently in the West Antarctic Rift System. This rift system is the deepest in the world (LeMasurier, 2008) and

accommodated extension in Cretaceous to Cenozoic time (Granot and Dyment, 2018).

The Antarctic Peninsula, including the South Orkney microcontinent, evolved since the Late Paleozoic as a long-lived active continental margin related to (paleo-)Pacific subduction, and hosts a discontinuous record of Jurassic-Paleogene arc magmatism intruding continental rocks that were autochthonous to the Gondwana margin (Burton-Johnson and Riley, 2015; Jordan et al., 2020; Navarrete et al., 2019, and references therein). The western margin dominantly consists of convergent margin successions, including a Lower Jurassic to Lower Cretaceous accretionary complex (Doubleday et al., 1993; Suárez, 1976), overlain by an Upper Jurassic to mid-Cretaceous fore-arc succession (Butterworth et al., 1988). The eastern margin of the Antarctic Peninsula is characterised by Jurassic-Cretaceous magmatism, including the 188–153 Ma Chon Aike silicic Large Igneous Province (Pankhurst et al., 2000; Riley and Knight, 2001), and volcanic and sedimentary successions related to continental and ocean basin extension during Gondwana break-up (Hathway, 2000; Willan and Hunter, 2005). The mid-Cretaceous to Cenozoic geology of Antarctic Peninsula is characterised by subduction-related arc magmatism that ended before the Late Neogene, followed by extension-related Neogene to recent intraplate alkaline volcanic rocks (Burton-Johnson and Riley, 2015).

3. Approach

3.1. Methods

We review deformational records from Patagonia and the Antarctic Peninsula to build a geometrically consistent reconstruction using the freely available software package, GPlates (www.gplates.org; Boyden et al., 2011), based on published quantitative kinematic constraints. All reconstruction files are provided in the Supplementary Information (rotation files and shapefiles). We apply a reconstruction hierarchy for active margin reconstructions previously used for the Caribbean (Boschman et al., 2014), SW Pacific (van de Lagemaat et al., 2018), NW Pacific (Vaes et al., 2019), and Mediterranean regions (Van Hinsbergen et al., 2020). This hierarchy ensures that the philosophy behind all regional reconstructions is identical and can be integrated into a global model, and that reconstructions are reproducible and adaptable when new data become available. We only use input data that provide direct information on relative (plate) motion, with uncertainty increasing at every step of the hierarchy (Boschman et al., 2014; Van Hinsbergen et al., 2020): first, extensional records are used, which are the most complete at the end of a tectonic event and thus provide the most reliable source of information for kinematic evolution. The primary data type used in our reconstruction is Euler rotations computed from marine magnetic anomalies and fracture zones. Our preferred data type thus comes from oceanic basins with active seafloor spreading. GPlates interpolates motion between constrained stages assuming constant rotation rate, thus allowing use of all available anomaly picks for the various ocean basins. Our reconstruction uses the timescale of Gradstein et al. (2012) that intercalibrated ages of the marine magnetic anomaly isochrons with biostratigraphy. Second, we use geological and geophysical data that allow estimating the timing and magnitude of rift records. These records are predominantly derived from intracontinental extensional settings but in some cases come from intra-oceanic rift settings. Third, intracontinental strike-slip and transform records are used. These accurately constrain the motion direction, but the amount of displacement may have higher uncertainty. Fourth, we use shortening records, which provide only a minimum estimate of convergence because part of the deformation record may be lost (e.g. Schepers et al., 2017).

The geometries of our tectonic blocks were drawn based on the approximate present-day locations of continent-ocean transitions, using a digital elevation model. The geometries of the tectonic blocks are shown in Fig. 1. Our boundaries may differ slightly from the recently mapped block boundaries that Beniest and Schellart (2020) defined. However, because the continental fragments of the Scotia Sea have all been extended during rifting preceding oceanic spreading, their shapes and areas have been strongly deformed and the modern shapes will overlap in the reconstruction.

3.2. Reconstruction approach

To restore where the (proto-)South Sandwich subduction zone(s) initiated, we first restore motion along the Magallanes-Fagnano shear zone, shortening in the Magallanes fold-and-thrust-belt, and extension documented from marine magnetic anomalies in the Scotia Sea oceanic basins (Figs. 1 and 4). This reconstruction will provide the tectonic configuration of the Scotia Sea region at the onset of oceanic crust formation in the latest Eocene (~36 Ma). Assessing intracontinental extension preceding oceanic spreading ('pre-drift extension') is challenging given the paucity of geological and geophysical data. We estimate the amount of pre-drift extension within southern South America by reconstructing the area that was occupied by South American oceanic lithosphere conjugate to the Weddell Sea prior to South Sandwich subduction. The locations of the restored anomalies on the South American Plate are based on the relative motion between the East Antarctic and South American plates. This follows from a plate circuit through Africa that we develop by reconstructing spreading at the South Atlantic and

Southwest Indian mid-ocean ridges based on constraints reviewed in section 4.2. The overlap between the South American conjugate lithosphere of the Weddell Sea on the one hand, and the restored latest Eocene configuration of Scotia Sea continental fragments on the other hand then provides an estimate of the amount of pre-drift extension. We use this estimate to restore the continental fragments to a location closer to Tierra del Fuego to avoid overlap of these fragments with South American oceanic crust that formed the conjugate to Weddell Sea.

Next, we use the plate circuit through Africa to evaluate whether convergence occurred between Tierra del Fuego and the Antarctic Peninsula in the Drake Passage region that may have started (proto-) South Sandwich subduction. However, this first requires restoring any intra-South American deformation between Tierra del Fuego and the South Atlantic margin and between the Antarctic Peninsula and East Antarctica. The Antarctic Peninsula is geographically part of West Antarctica, and it has been suggested that the West Antarctic Rift System, forming the plate boundary between East and West Antarctica, continues into the Weddell Sea (Dalziel, 2006). This would render the Antarctic Peninsula also tectonically part of West Antarctica. Based on paleomagnetic studies, however, most authors interpret the Antarctic Peninsula as rigidly attached to East Antarctica since at least the mid-Cretaceous (Bakhmutov and Shpyra, 2011; Gao et al., 2018; Grunow, 1993; Milanese et al., 2019; Milanese et al., 2017; Poblete et al., 2011; Watts et al., 1984).

3.3. Paleomagnetic data selection

We use a newly compiled paleomagnetic database (provided in the Supplementary Information) for the Antarctic Peninsula and southern South America to test, and if necessary, iteratively improve, our kinematic reconstruction. To this end, we use the online paleomagnetic analysis platform Paleomagnetism.org (Koymans et al., 2020; Koymans et al., 2016). This platform includes a tool that allows to predict the Global Apparent Polar Wander Path (for which we use the version of Torsvik et al. (2012) in the coordinates of any restored block in GPlates (see Koymans et al., 2020; Li et al., 2017). We compiled paleomagnetic data derived from Lower Jurassic to Eocene volcanic and sedimentary rocks of the Antarctic Peninsula, and southernmost South America. We use the criteria for data selection defined by Lippert et al. (2014) and Li et al. (2017), by which we exclude data that 1) are not used in the original publication if the reason for this exclusion was provided; 2) are (likely) remagnetised according to the original authors; 3) contain lava sites of mixed polarity, as spot readings cannot record reversals; 4) consist of less than 3 samples sedimentary sites or less than 3 lava sites for igneous rocks; 5) do not adequately sample paleosecular variation, using the criteria of Deenen et al. (2011).

To include as much information from the sparse record of paleomagnetic data as possible, published data is included in the database if at least 3 lava sites are present in close contact and these were interpreted by the original authors as primary magnetic directions. We thereby apply somewhat less stringent quality criteria compared to those of Meert et al. (2020), who argue for a minimum of 8 sites. We color-coded the paleomagnetic data based on the quality of the paleomagnetic dataset. Mean directions based on 8 sites or more are plotted in green, unless the Fisher (1953) precision parameter of the distribution of VGPs falls outside of $10 \leq K \leq 70$ (following the quality criteria of Meert et al., 2020), in which case the mean direction is plotted in orange. Mean directions based on fewer than 8 sites are plotted in red. Datasets obtained from (clastic) sedimentary rocks are known to be prone to inclination shallowing (e.g., King, 1955; Tauxe and Kent, 2004) and are thus not suitable to provide estimates of the inclination and paleolatitude, unless corrected for the effects of inclination shallowing (e.g., Vaes et al., 2021). We used the available sedimentary datasets only to test the paleomagnetic declination as predicted by our reconstruction (plotted in blue; Figs. 5 and 7). The only published inclination shallowing-corrected dataset for these regions is from a magnetostratigraphic study of Upper
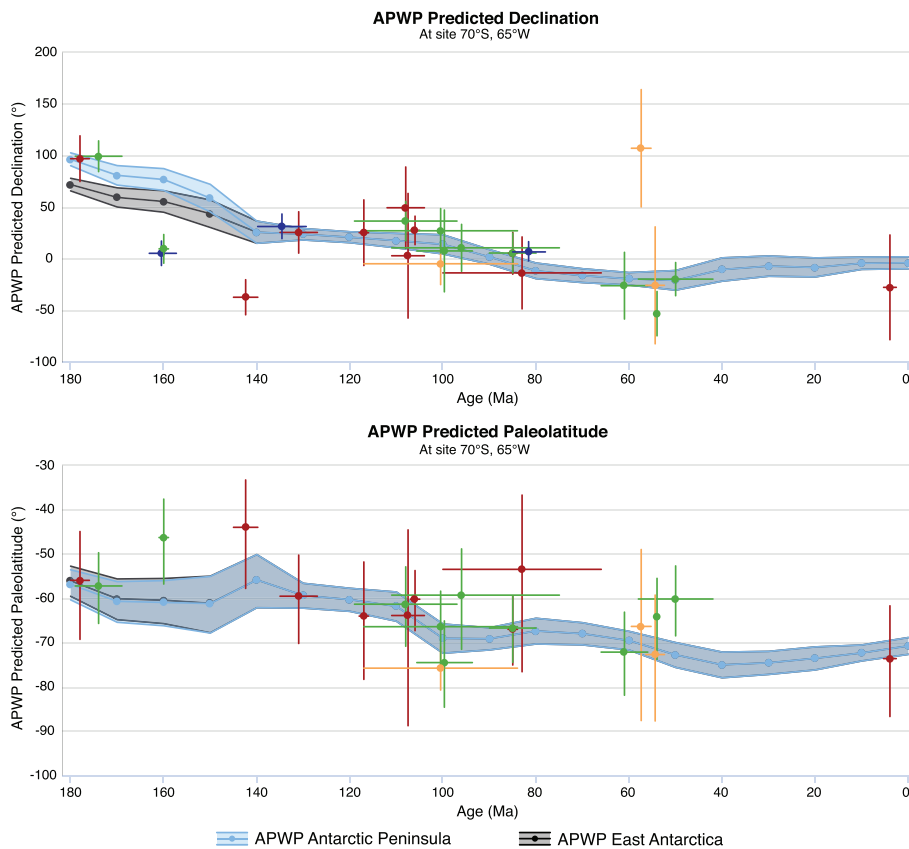
Fig. 5. Paleomagnetic declination (top) and predicted paleolatitude (bottom) data from the Antarctic Peninsula plotted against our reconstructed declination/paleolatitude curves for East Antarctica (black line) and the Antarctic Peninsula (blue line) relative to a reference point on the Antarctic Peninsula (70°S, 65°W). The color of the volcanic data point represents their quality, based on the quality criteria of Meert et al. (2020). Green = $N \geq 8$ and $10 \leq K \leq 70$; Orange = $N \geq 8$ and $K < 10$ or $K > 70$. Red = $N < 8$. Blue data points are from sedimentary sites which all have $N \geq 8$ and $10 \leq K \leq 70$. Due to the potential effects of inclination flattening we only use sedimentary sites for declination (see also section 3.3).

Cretaceous clastic sediments from Ross Island, by Milanese et al. (2019). We evaluated the reliability of their two results (NW and SE Ross Island) using the recently defined reliability criteria of Vaes et al. (2021). The anomalously large scatter of the individual directions ($K < 8$) suggests that the distribution of directions, even after the application of a data cut-off, is contaminated by a significant contribution of noise that is unrelated to paleosecular variation. Consequently, the application of the reliability criteria yields a quality grade 'C' for these datasets, indicating that the datasets do not provide a robust estimate of the inclination and associated paleolatitude (Vaes et al., 2021).

4. Review

We present here an overview of the quantitative kinematic constraints that are used as input for our reconstruction. First, we review the Scotia Sea region itself, delineated by the Shackleton Fracture Zone, the Magallanes-Fagnano Fault Zone and North Scotia Ridge, the South Sandwich Trench, and the South Scotia Ridge (Fig. 1). The Scotia Sea region is mainly underlain by oceanic crust, which means that these data come from marine magnetic anomalies, corresponding to step 1 of our reconstruction hierarchy, as outlined in section 3.2. Second, we review constraints on the South America-Africa-Antarctica plate circuit from the South Atlantic and Southern oceans and the Weddell Sea, corresponding to steps 1 (oceanic spreading) and 2 (pre-drift extension) of our reconstruction hierarchy. Third, we review geological and paleomagnetic constraints on deformation within Antarctica and South America to tie Tierra del Fuego and the Antarctic Peninsula to the plate circuit. This part includes data from steps 3 (strike-slip and transform motion), 4 (intracontinental compression), and 5 (paleomagnetic constraints) of the reconstruction hierarchy.

4.1. Scotia Sea

Seafloor spreading in the East Scotia Basin is recorded by marine magnetic anomalies that are mirrored either side of the East Scotia Ridge (Fig. 4). West of the ridge, anomalies go back to C5C (17 Ma; Larter et al., 2003), but on the eastern side, the oldest identifiable magnetic anomaly is C4A (9.1 Ma; Larter et al., 2003). The South Sandwich Arc has likely intruded and overlain the older anomalies (Vanneste and Larter, 2002). The Central Scotia Basin hosts *E*-W trending anomalies (Fig. 4) suggesting N-S paleo-spreading of unknown age, either related to Cenozoic Scotia Sea extension (Livermore et al., 2007), or representing a relic of Mesozoic South American conjugate lithosphere of Weddell Sea (Eagles, 2010). Since there is no fossil spreading ridge identified (Dalziel et al., 2013), we will evaluate both possibilities in the reconstruction section. The West Scotia Basin occupies most of the Scotia Plate and hosts an extinct mid-ocean ridge with a well-defined, symmetric set of magnetic anomalies (Eagles et al., 2005). The identification of marine magnetic anomalies C8-C5 (Fig. 4) indicates that spreading started before ~26.0 Ma and ceased during chron C3An (~6.1 Ma; Eagles et al., 2005). However, some studies postulated the existence of older anomalies in the western part of the basin, with ages corresponding to chrons C10 or C12 (~28–30.5 Ma; Livermore et al., 2005; Lodolo et al., 2006). The identified anomalies older than C8 are of low amplitude and are interpreted as disorganised early stages of seafloor spreading that started around 32–30 Ma (Eagles et al., 2005; Livermore et al., 2005; Lodolo et al., 2006).

In the South Scotia Ridge, the Scan Basin between the Discovery and Bruce Banks contains NNW-SSE anomalies from chrons C16n.1n-C11n.2n, with ages ranging from ~35.7–29.5 Ma (Schreider et al., 2017). The Dove Basin between the Bruce and Pirie Banks contains a NNE-SSW elongated ridge that is close to the axis of the basin flanked by marine magnetic anomalies corresponding to chrons C6Cn.2n-C6Ar (23.0–20.7 Ma; Schreider et al., 2018), in correspondence with 20.4

± 2.6 to 22.8 ± 3.1 Ma whole-rock ^{40}Ar/^{39}Ar ages of dredged MORB samples (Galindo-Zaldívar et al., 2014). Schreider et al. (2018) tentatively interpreted additional anomalies located in the eastern part of the Dove Basin as C8n.1n-C6Cr (23.3–25.3 Ma). These presumably formed during an earlier phase of slow spreading, after which the spreading ridge jumped westwards (Schreider et al., 2018). The Protector Basin between the Pirie Bank and the Terror Rise contains north-south oriented marine magnetic anomalies corresponding to chrons C5Dn-C5ABr (17.5–13.6 Ma; Galindo-Zaldívar et al., 2006; Schreider et al., 2018). To the south, the narrow Jane Basin between the Jane Bank and the South Orkney microcontinent has marine magnetic anomalies interpreted to have formed during chrons C5Dn-C5ADn (17.5–14.2 Ma; Bohoyo et al., 2002). Finally, the Powell Basin between the Antarctic Peninsula and the South Orkney microcontinent contains an extinct spreading ridge with NW-SE striking marine magnetic anomalies corresponding to chrons C11-C6AA (29.5–21.2 Ma; Fig. 4; Eagles and Livermore, 2002).

4.2. South America – Africa – East Antarctica plate circuit

The oldest identified anomaly in the South Atlantic Ocean that records spreading between South America and Africa north of the Falkland Plateau (Fig. 3) is M4 (e.g. König and Jokat, 2006), indicating that seafloor spreading has been active since at least ~131 Ma (Gradstein et al., 2012). Cretaceous opening of the South Atlantic in our reconstruction follows Gaina et al. (2013), but converted to the timescale of Gradstein et al. (2012). There are several pre-breakup fits for the South Atlantic region that differ by a few degrees, and these variably advocate for strike-slip fault zones cutting South America into several tectonic blocks, which were active during pre-drift extension before the onset of seafloor spreading (Heine et al., 2013; Moulin et al., 2010; Pérez-Díaz and Eagles, 2014; Torsvik et al., 2009). Recently, Owen-Smith et al. (2019) tested the different full-fit reconstructions of Africa and South America against paleomagnetic data of the Paraná (South America)-Etendeka (Africa) Large Igneous Province that is thought to have sparked the South Atlantic opening. They concluded that the reconstruction of Torsvik et al. (2009) provides the best fit to the paleomagnetic data, and therefore we use the deformation zones and finite rotation poles for the pre-breakup fit from Torsvik et al. (2009), with the exception of the Gastre Fault, which we review separately in section 4.3. The fit of Torsvik et al. (2009) contains ~50–180 km pre-drift extension between southern South America and Africa, and ~ 120–600 km between northern South America and Africa, occurring from 138 Ma, before true seafloor spreading established at ~131 Ma (whereby we converted ages to the Gradstein et al. (2012) timescale).

Antarctica, as part of East Gondwana, broke away from Gondwana in the Jurassic, which preceded the break-up of West Gondwana into Africa and South America. The separation of East Gondwana from West Gondwana is constrained by marine magnetic anomalies of the Southwest Indian Ridge (Fig. 1) identified by Royer and Chang (1991), Bernard et al. (2005), Cande et al. (2010), and Mueller and Jokat (2019). The oldest marine magnetic anomaly between Africa and East Antarctica was interpreted as M38n2n (~164 Ma; Mueller and Jokat, 2019). Pre-drift extension between East and West Gondwana was estimated to have started at ~182 Ma, coincident with the initial emplacement of flood basalts of the Karoo-Ferrar Large Igneous Province on both margins (Mueller and Jokat, 2019).

The combined South Atlantic and Southern Ocean reconstructions constrain relative motion between East Antarctica and South America. Direct constraints on this motion are also available, in the Weddell Sea. However, the remote conditions, thick sedimentary cover, and the fact that only half of the ocean crust remains (the South American conjugate has largely subducted), means that the anomaly data are of lesser quality than for the South Atlantic and Southern Oceans. The oldest marine magnetic anomaly of the South America-Antarctica Ridge preserved on the South American Plate to the east of the South Sandwich trench is C31y (~68.4 Ma; Eagles, 2016a; Livermore et al., 2005). Older marine

magnetic anomalies are only preserved on the Antarctic Plate in the Weddell Sea (Fig. 4). These are interpreted to become younger towards the north, but their age is debated (Barker and Jahn, 1980; Barker et al., 1984; LaBrecque and Barker, 1981; Livermore and Woollett, 1993). Eagles (2016a) identified M14o (~138 Ma) as the oldest isochron, while Jokat et al. (2003) proposed an onset of seafloor spreading at M24 (~154 Ma). Ghidella et al. (2002) suggested an even older but tentative start of seafloor spreading at ~160 Ma based on adjusting synthetic isochrons to seafloor spreading lineations and flow lines. Previously proposed pre-drift extension ages include ~167 Ma based on the extrapolation of spreading rates derived from subsequent marine magnetic anomalies (König and Jokat, 2006). These rates are used to restore pre-drift extension between South America and Antarctica back into the Gondwana fit (König and Jokat, 2006). An Early Jurassic onset of pre-drift extension has also been proposed based on arc extension in the Antarctic Peninsula (Storey et al., 1996). The most recent estimate, and the one used in our reconstruction, is of Mueller and Jokat (2019) who dated the start of pre-drift extension at ~182 Ma, based on ship-borne magnetic data, immediately following the emplacement of the Ferrar Large Igneous Province.

4.3. Deformation within South America

At present, deformation in southern South America is focused along the Magallanes-Fagnano fault zone (Fig. 1). About 20–80 km of left-lateral strike-slip motion was estimated, with a minor (up to ~10 km) normal slip component (Klepeis, 1994a; Lodolo et al., 2003; Pelayo and Wiens, 1989; Torres-Carbonell et al., 2008a). Field observations and seismic data reveal that structures related to left-lateral strike-slip motion consistently crosscut contractional structures of the Magallanes fold-and-thrust belt (e.g. Betka et al., 2016; Klepeis, 1994a; Klepeis and Austin Jr., 1997). The onset of strike-slip motion is thought to be related to either the start or end of West Scotia Sea spreading; i.e. late Oligocene (Klepeis and Austin Jr., 1997) or late Miocene (Lodolo et al., 2006). Based on balanced cross-sections, the latest phase of contractional deformation in the Magallanes fold-and-thrust belt occurred in the latest Oligocene to early Miocene (Torres-Carbonell et al., 2011; Torres-Carbonell et al., 2008b). A maximum early Miocene age is therefore inferred for the onset of strike-slip motion along the Magallanes-Fagnano fault system (Betka et al., 2016), which corresponds to widespread uplift and exhumation in the region measured through low-temperature thermochronology (Fosdick et al., 2013). Based on displaced markers, Torres-Carbonell et al. (2008a) estimate ~50 km of sinistral strike-slip motion since the late Miocene. This age corresponds to the ~7 Ma onset of folding in the Falkland Trough, the offshore continuation of the South America-Scotia plate boundary (Esteban et al., 2020).

Shortening in the Magallanes fold-and-thrust belt occurred between mid-Cretaceous and early Miocene time (Klepeis et al., 2010; Torres-Carbonell et al., 2013; Torres-Carbonell et al., 2014). The onset of shortening in the mid-Cretaceous is related to the final closure of the Rocas Verdes Basin (Klepeis et al., 2010). The youngest rocks infilling the Rocas Verdes Basin are Albian (Dott et al., 1977), and the oldest flysch related to closure was deposited during the Albian to Cenomanian (Scott, 1966; Wilson, 1991). Foreland basin deposits following closure are dated at ~101–88 Ma based on U-Pb detrital zircon analysis (Fildani et al., 2003; Fosdick et al., 2011; McAtamney et al., 2011), although the initiation of thrusting probably occurred earlier (Calderón et al., 2007). During the Late Cretaceous and into the Cenozoic convergence continued and the deformation front migrated towards the foreland (Fosdick et al., 2011; Torres-Carbonell and Dimieri, 2013; Torres-Carbonell et al., 2013; Torres-Carbonell et al., 2011; Torres-Carbonell et al., 2008b). The Cenozoic phase of shortening was restored using balanced cross-sections, and here we follow the reconstruction of Schepers et al. (2017). Those authors restored a total of 50–80 km of Cenozoic shortening in the southern Patagonian and the Fuegian Andes based on estimates of Kley et al. (1999), Kraemer (1998), Ghiglione et al. (2014),

Fosdick et al. (2011), Betka (2013), and Klepeis et al. (2010). In addition, based on a structural restoration of a deformed geological cross section, Fosdick et al. (2011) infer that 32–40 km of pre-Cenozoic shortening occurred in the Magallanes fold-and-thrust belt following the final closure of Rocas Verdes Basin around 100 Ma, of which about 27 km occurred between 88 and 74 Ma.

Quantifying the amount of shortening related to Rocas Verdes Basin closure is more difficult due to absence of markers and loss of lithosphere through subduction related to closure of the basin (Klepeis et al., 2010). South directed subduction led to the consumption of oceanic crust of the Rocas Verdes Basin below the Pacific margin of Patagonia, which hosts the Patagonian batholith (Klepeis et al., 2010). The width of the basin is debated, and estimates mostly range between 100 and 300 km based on field, geochemical, and paleomagnetic arguments (Burns et al., 1980; Dalziel, 1981; De Wit, 1977; de Wit and Stern, 1981). Winn Jr (1978) proposed a maximum width of 300 km in Tierra del Fuego as the basin was filled with moderately coarse deep-sea fan sediments, which are unlikely to have been deposited if the basin edges were farther away. Kraemer (2003) estimated a minimum of 300 km and a maximum of 600 km of shortening across the entire southern Andes orogen since the Cretaceous. He attributed a maximum amount of 430 km to mid-Cretaceous shortening, of which 230 km was considered to be related to the mid-Cretaceous closure of the Rocas Verdes Basin, and 200 km to thick-skinned tectonics in the Cordillera Darwin (Kraemer, 2003). The age of opening of the Rocas Verdes Basin is estimated to be Late Jurassic to Early Cretaceous based on zircon U-Pb geochronology of ophiolitic rocks. These yielded ages of 139 ± 2 Ma in Patagonia (Stern et al., 1992) and 150 ± 1 Ma on South Georgia (Mukasa and Dalziel, 1996; Fig. 3). Additionally, Calderón et al. (2007) used magmatic and detrital zircon U-Pb geochronology to date volcanism and rifting in the basin, which occurred between at least ~152 to 142 Ma.

For South America north of the southernmost Andes, we adopt the finite rotation poles of Schepers et al. (2017) for Cenozoic deformation in the Andes, and of Torsvik et al. (2009) for strike-slip deformation related to South America-Africa pre-drift extension. A controversial element in the latter reconstruction is the ~500 km of dextral strike-slip motion that is proposed to be accommodated on the Gastre Fault between initial breakup (182 Ma) and the onset of oceanic spreading (134 Ma). The Gastre Fault System (Fig. 1) as a major Jurassic tectonic boundary was first proposed by Rapela and Pankhurst (1992), based on significant changes in geology across the shear zone, and scattered outcrops of mylonites and cataclasites with a NW-SE striking foliation that are thought to confirm the existence of a shear zone. Several kinematic reconstructions include dextral motion on this fault to create space for the Antarctic Peninsula outboard of Patagonia in Gondwana reconstructions (Dalziel et al., 2000; König and Jokat, 2006; Macdonald et al., 2003). Additionally, Schimschal and Jokat (2019) recently used seismic data to identify Jurassic extension in the Falkland Plateau between Maurice Ewing Bank and the Falkland Islands, which occurred between ~178 and 154 Ma. This extension requires almost 500 km of dextral motion on the Gastre Fault during the same period to avoid crustal gaps and overlaps of continental crust. However, whether the Gastre Fault System served as a major dextral shear zone remains debated (e.g., González et al., 2020) as unequivocally demonstrating its presence in the field proves challenging (Von Gosen and Loske, 2004; Zaffarana et al., 2010; Zaffarana et al., 2017).

4.4. Deformation within Antarctica

To use the South Atlantic plate circuit to constrain relative motion between southern South America and the Antarctic Peninsula, it is crucial to establish whether the Antarctic Peninsula was tectonically part of East Antarctica or West Antarctica. The Antarctic Peninsula is bounded in the south by the Ferrigno Rift that separates it from Thurston Island (Bingham et al., 2012), and in the southeast by the Evans Rift that separates it from the Ellsworth-Whitmore Mountains (Jones et al., 2002;

Fig. 3). There are no estimates on the magnitude and timing of displacement along these rifts, but one of these rifts may have served as the continuation of the West Antarctic Rift System (WARS), which formed the plate boundary between East and West Antarctica.

It is commonly accepted that the continuation of the WARS was located between the Antarctic Peninsula and Thurston Island and that the Antarctic Peninsula has been tectonically part of East Antarctica since at least the Early Cretaceous (Bingham et al., 2012; Eagles et al., 2009; Gohl et al., 2007; Jordan et al., 2010; Müller et al., 2007). Dalziel (2006), however, proposed that the WARS connects the Ross Sea with the Weddell Sea, which would imply that the Antarctic Peninsula is tectonically part of West Antarctica. In this setting, relative motion between the Antarctic Peninsula and East Antarctica may have occurred until the Miocene, based on marine magnetic anomalies from the Northern and Adare Basins that constrain motion in the WARS (Cande et al., 2000; Fitzgerald and Baldwin, 1997; Granot et al., 2013; Granot and Dyment, 2018; Luyendyk et al., 2001).

We use paleomagnetic data from the Antarctic Peninsula to evaluate whether the peninsula was tectonically part of West Antarctica or East Antarctica in the Mesozoic and Cenozoic. We plotted the declination and paleolatitude of these sites (Fig. 5), rotated to East Antarctic coordinates for a reference point on the Antarctic Peninsula (70°S, 65°W), against the Global Apparent Polar Wander Path (GAPWaP) of Torsvik et al. (2012). The paleomagnetic data of the Antarctic Peninsula are in good agreement with the predicted GAPWaP for the last ~145 Ma (Fig. 5). Based on these paleomagnetic constraints, there is no reason to assume any relative motion between the Antarctic Peninsula and East Antarctica since the Early Cretaceous. In our reconstruction the Antarctic Peninsula is tectonically part of East Antarctica, which is in agreement with earlier conclusions (Bakhmutov and Shpyra, 2011; Gao et al., 2018; Grunow, 1993; Milanese et al., 2019; Milanese et al., 2017; Poblete et al., 2011; Watts et al., 1984).

5. Reconstruction

5.1. Early Jurassic – Late Cretaceous

Our reconstruction (see Supplementary Information for GPlates files) starts at 182 Ma (Fig. 6a), when East Gondwana (Antarctica, Australia, Zealandia, India) started to separate from West Gondwana (South America, Africa; Mueller and Jokat, 2019). Shortly after the onset of pre-drift extension between Africa and Antarctica, extension started at 178 Ma between the Falkland Islands and Maurice Ewing Bank, creating the Falkland Plateau Basin (Schimschal and Jokat, 2019). During this time, the Maurice Ewing Bank remained in a fixed position relative to Africa, and we restore 450 km of extension in the Falkland Plateau that is accommodated by right-lateral strike-slip motion in South America along the Gastre Fault (Schimschal and Jokat, 2019). Both the extension in the Falkland Plateau Basin and strike-slip motion along the Gastre Fault ceased at 154 Ma (Fig. 6b; Schimschal and Jokat, 2019).

After 300–500 km of pre-drift extension, seafloor spreading between Antarctica and Africa was established around 160 Ma (Mueller and Jokat, 2019) and caused an increase in divergence rates between East and West Gondwana. The increase in relative plate motion was concurrent with extension on the western margin of Gondwana. Subsequently, at 154 Ma, the Rocas Verdes Basin started opening (Calderón et al., 2007) and simultaneously, clockwise rotation of the Antarctic Peninsula relative to East Antarctica commenced (Figs. 6b and 5c). This rotation is consistent with paleomagnetic data and is required to avoid overlap between the Antarctic Peninsula and Patagonia in the Gondwana reconstruction (Grunow, 1993; Longshaw and Griffiths, 1983; Figs. 5a and 6a). The restoration of the Antarctic Peninsula outboard of Patagonia provides a straightforward explanation for why there is widespread pre-Late Jurassic arc magmatism due to Phoenix subduction below Gondwana on the Antarctic Peninsula and north of the Rocas Verdes Basin, but not in southern Patagonia (Navarrete et al., 2019).
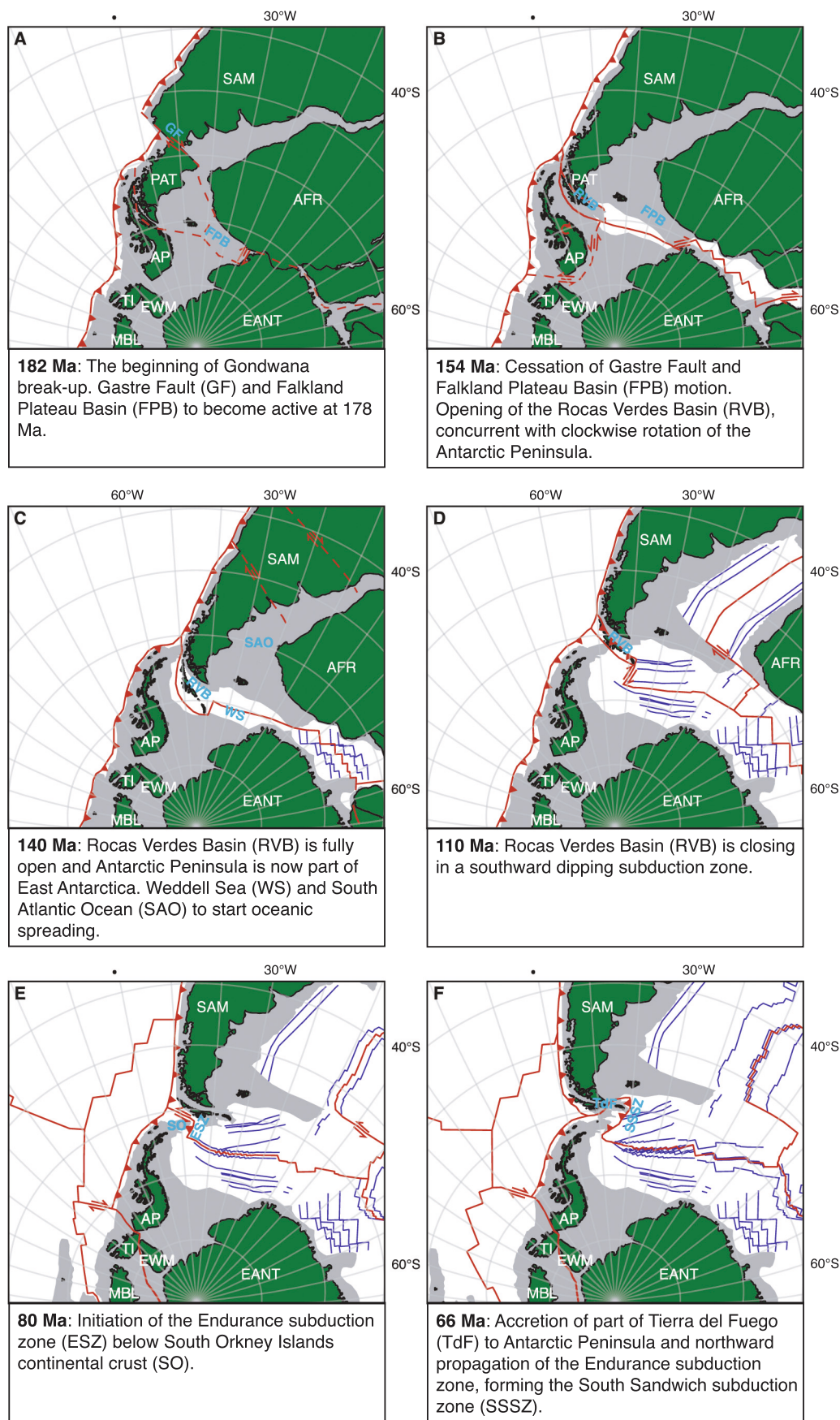
Fig. 6. Snapshots of the kinematic reconstruction at selected time slices in an East Antarctica fixed reference frame. Dark green areas represent present-day coastal boundaries of the polygons, dark gray areas represent stretched and transitional continental crust. Red lines represent active plate boundaries, red arrows represent motions on the active plate boundaries. Dashed red lines are plate boundaries that are to become active soon after the reconstruction snapshot. Dark blue lines are marine magnetic anomaly lineations. The oceanic basins west of South America and Antarctica are not reconstructed, and therefore no marine magnetic anomalies are shown, plate boundaries in this region are given for reference and are based on the reconstruction of Müller et al. (2019).

A 182 Ma: The beginning of Gondwana break-up. Gastre Fault (GF) and Falkland Plateau Basin (FPB) to become active at 178 Ma.

B 154 Ma: Cessation of Gastre Fault and Falkland Plateau Basin (FPB) motion. Opening of the Rocas Verdes Basin (RVB), concurrent with clockwise rotation of the Antarctic Peninsula.

C 140 Ma: Rocas Verdes Basin (RVB) is fully open and Antarctic Peninsula is now part of East Antarctica. Weddell Sea (WS) and South Atlantic Ocean (SAO) to start oceanic spreading.

D 110 Ma: Rocas Verdes Basin (RVB) is closing in a southward dipping subduction zone.

E 80 Ma: Initiation of the Endurance subduction zone (ESZ) below South Orkney Islands continental crust (SO).

F 66 Ma: Accretion of part of Tierra del Fuego (TdF) to Antarctic Peninsula and northward propagation of the Endurance subduction zone, forming the South Sandwich subduction zone (SSSZ).

Fig. 6. (*continued*).

G

50 Ma: Start of overriding plate extension above the South Sandwich subduction zone (SSSZ). Separation of continental lithosphere fragments from South America and Antarctic Peninsula.

H

36 Ma: Onset of oceanic crust formation in the overriding plate above the South Sandwich subduction zone, starting in the Central Scotia Sea (CSS) and Scan Basin (SB).

I

26 Ma: Complicated plate boundary setting in the Scotia Sea with multiple spreading ridges active simultaneously.

J

15 Ma: Arrival of segments of the South America-Antarctica Ridge (SAAR) in the southern segment of the South Sandwich subduction zone (SSSZ) and progressive shutdown of this part of the trench.

K

Present: Present day setting of the Scotia Sea region with active back-arc spreading in the East Scotia Sea (ESS).

Following opening of the Rocas Verdes Basin, extension occurred along the eastern margin of Antarctica (Storey et al., 1996). Meanwhile, extension was also accommodated in the Weddell Sea between Antarctica and South America, where seafloor spreading was established around 140 Ma (Eagles, 2016a). This time marks the end of opening of the Rocas Verdes Basin (Calderón et al., 2007; Fig. 5c). The end of rotation of the Antarctic Peninsula in our reconstruction coincides with the end of Rocas Verdes Basin opening at 140 Ma (Fig. 6c).

Pre-drift extension between South America and Africa preceding the opening of the South Atlantic Ocean started around 135 Ma (Torsvik et al., 2009), and the onset of seafloor spreading was around the time of magnetic anomaly M4 (~131 Ma; König and Jokat, 2006). A clockwise rotation of Antarctica relative to South America and Africa occurred during the mid-Cretaceous. The exact timing is uncertain due to lack of polarity reversals during the Cretaceous Normal Superchron (~125.9–83.6 Ma; Gradstein et al., 2012), but is evidenced from a bend in fracture zones of the Weddell Sea (König and Jokat, 2006) and Southwest Indian Ocean (Mueller and Jokat, 2019). In the western Weddell Sea region, the rotation of Antarctica caused a change in relative motion between Tierra del Fuego and the Antarctic Peninsula: from the extensional phase since Gondwana break-up, to a period of transcurrent motion (~125–113 Ma), and then to a phase of convergence between ~113–102 Ma. The timing of these changes in relative plate motion is based on synthetic flowlines to fit fracture zones of the Southwest Indian Ridge, as marine magnetic anomalies are absent (Mueller and Jokat, 2019). The change in relative plate motion led to oblique convergence between the Antarctic Peninsula and the Pacific margin of the Rocas Verdes Basin, which is thought to have led to closure of the Rocas Verdes Basin (Eagles, 2016a). In addition, this change in plate motion is proposed to have led to closure of a whole series of back-arc basins that were present along the western margin of South America south of 5°S (Dalziel, 1986). The change in plate motions allows for closure of the Rocas Verdes Basin between 113 and 102 Ma, in line with the ages of overlying flysch sediments (Scott, 1966; Wilson, 1991) and the formation of the fold-and-thrust belt (Fosdick et al., 2011), which we adopt in our reconstruction (Fig. 6d).

5.2. Width of the Rocas Verdes Basin

The width of the Rocas Verdes Basin is difficult to constrain, as no quantitative kinematic constraints are available. To assess the effects of minimum and maximum basin widths, we created two end-member
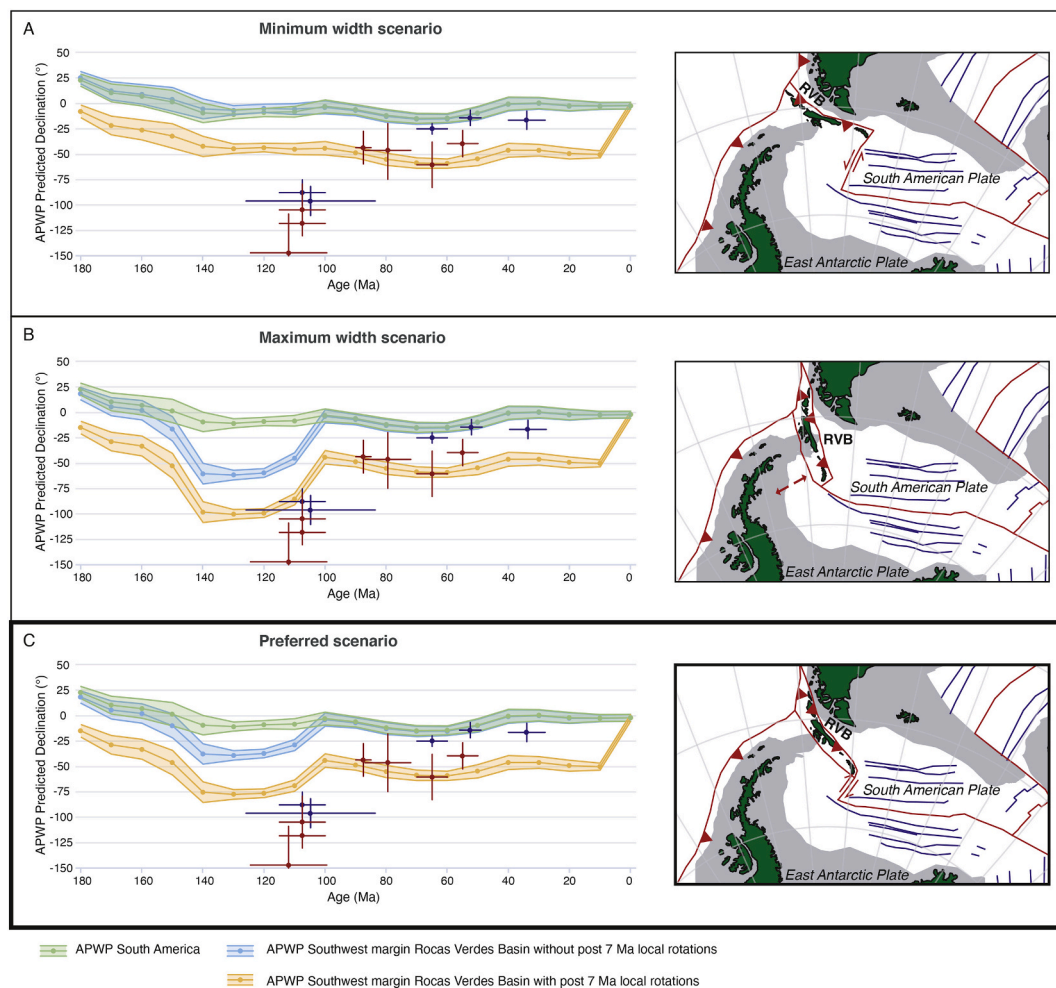
Fig. 7. Paleomagnetic declination data from Tierra del Fuego plotted against declination curves of South America (green line) and the southwest margin of the Rocas Verdes Basin (blue line) relative to a reference point in Tierra del Fuego (55°S, 65°W). The yellow line is the APWP of the southwest margin of the Rocas Verdes Basin that includes post 7 Ma rotations related to strike-slip tectonics (see Section 5.2). Red data points are from igneous sites with less than 8 samples, blue data points are from sedimentary sites. The different plots show the declinations curves of the different width scenarios of Rocas Verdes Basin, as explained in Section 5.2. On the right: snapshots at 113 Ma of the different scenarios for the maximum width of the Rocas Verdes Basin just prior to closure.

scenarios (Fig. 7). We tested these against paleomagnetic data, as the closure of the Rocas Verdes Basin may be related to the formation of the Patagonian orocline (Burns et al., 1980; Carey, 1955; Cunningham et al., 1991; Maffione, 2016; Maffione et al., 2010; Marshak, 1988). Declinations from the Tierra del Fuego region in southern Patagonia show counter-clockwise rotations up to ~100° between ~110 and 60 Ma, relative to the Global Apparent Polar Wander Path (GAPWaP) of Torsvik et al. (2012) in coordinates of the stable Amazonia Craton of South America, rotated into a reference point (55°S, 65°W) in southern South America (Fig. 7). These rotations have been associated with the Late Cretaceous closure of the Rocas Verdes Basin (Poblete et al., 2016) based on the systematic pattern of ~90° counter-clockwise rotated rocks of Early Cretaceous age (although paleomagnetic data is scarce) and ~ 35–50° counter-clockwise rotated rocks of Late Cretaceous and early Eocene age (Fig. 7). This would call for a ~ 40–55° rotation related to the closure of the Rocas Verdes Basin, and subsequent local rotations related to large sinistral strike-slip fault zones in the Tierra del Fuego region. Alternatively, the total rotations have been ascribed to strike-slip related deformation (Cunningham, 1993; Rapalini et al., 2015).

In the minimum width scenario, the basin is closed by the 113–102 Ma convergent motion between the Antarctic Peninsula and Tierra del Fuego only (Fig. 7a). This means that the south-western margin of the basin is rigidly attached to the Antarctic Peninsula during closure, which results in a 100–150 km wide basin. This scenario does not involve counter-clockwise rotation of the southwest margin of the Rocas Verdes Basin, thus suggesting that the paleomagnetic rotations are completely the result of local rotations related to strike-slip tectonics (Fig. 7a).

In the maximum width scenario, we open the Rocas Verdes Basin by the maximum clockwise rotation of the southwest margin of Patagonia relative to stable South America that does not lead to convergence between this margin and Antarctica. The resulting Rocas Verdes Basin in our reconstruction is up to 500 km wide (Fig. 7b). Subsequent closure leads to ~50° counter-clockwise rotation of the southwest margin of the Rocas Verdes Basin, which has a better fit with the Early Cretaceous paleomagnetic poles (Fig. 7b). The implication of the rotation, however, is that it results in up to 600 km extension between the eastern margin of the Antarctic Peninsula and the south-western margin of the Rocas Verdes Basin. In addition, the maximum width scenario causes overlap with South Orkney Islands continental crust. Because the minimum width scenario does not include the paleomagnetic rotations, we prefer a mixed model (Fig. 7c). In this model we reconstruct the closure of the Rocas Verdes Basin with the maximum counter-clockwise rotation that does not lead to overlap between the southwest margin of the Rocas Verdes Basin and South Orkney Islands continental crust. This mixed scenario involves a ~ 250 km wide Rocas Verdes Basin and accommodates about 25° counter-clockwise rotation during closure of the basin.
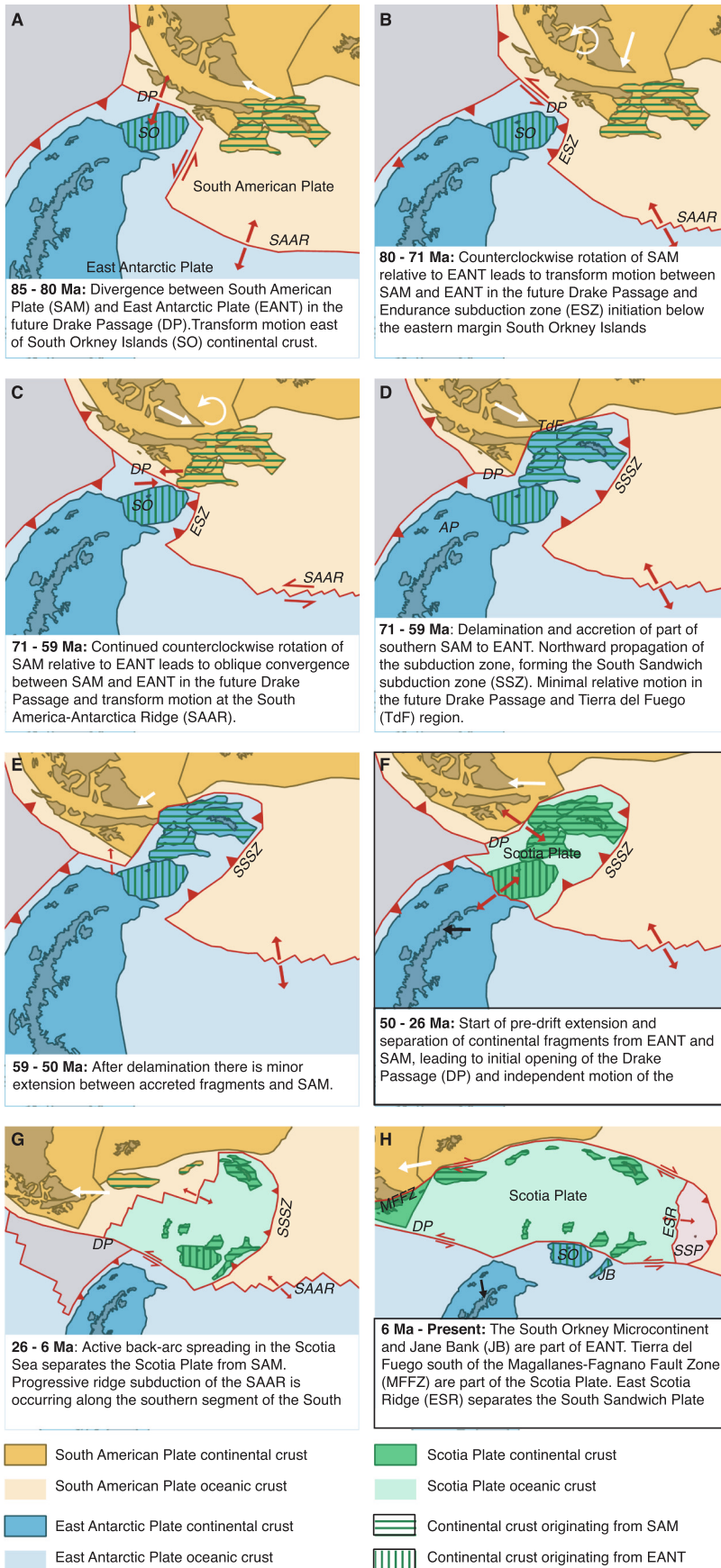
The Apparent Polar Wander Path (APWP) of the southwest margin of the Rocas Verdes Basin (blue line; Fig. 7) lies north of all paleomagnetic data points in all scenarios, which suggests additional counter-clockwise rotation after closure of the Rocas Verdes Basin. These post-Early Cretaceous rotations cannot be the result of a whole-block rotation of the southwest margin, however, as this does not fit geometrically. The additional rotation is therefore interpreted as the result of local rotations related to post 7 Ma counter-clockwise rotation associated with left-lateral strike-slip motion of the Magallanes-Fagnano fault zone. To illustrate how this fits better with paleomagnetic data, we plotted the APWP of a block that is part of the southwest margin of the Rocas Verdes Basin (Fig. 7c, yellow line), which underwent an additional 50° counter-clockwise rotation since 7 Ma. We note that there is only a very limited amount of paleomagnetic data available from Tierra del Fuego, and the quality of data available is generally poor. There is a need for more paleomagnetic data to get better constraints on the timing and amount of rotation in this region.

5.3. Late Cretaceous subduction initiation in the Scotia Sea region

After closure of the Rocas Verdes Basin, the Magallanes fold-and-thrust belt started forming in the Late Cretaceous, where shortening continued into the Neogene. Meanwhile seafloor spreading remained active in the Weddell Sea. Around 80 Ma, South America started moving westwards relative to Antarctica (Fig. 6e). This led to transcurrent motion in the future Drake Passage, where the Antarctica-Tierra del Fuego motion was accommodated along a transform system (Fig. 6e). Concurrently, shortening was renewed in the Magallanes fold-and-thrust belt (Klepeis et al., 2010; Fosdick et al., 2011). The Weddell Sea mid-ocean ridge, separating East Antarctica (including the Antarctic Peninsula) and South America, was still located southeast of the northern tip of the Antarctic Peninsula and South Orkney Islands continental crust. The mid-ocean ridge and the transform fault north of the Antarctic Peninsula were connected by a NE-SW striking plate boundary along the eastern margin of the Antarctic Peninsula and South Orkney Islands continental crust. This boundary was a transform fault during pre-80 Ma N-S extension in the Weddell Sea (Figs. 6d, 8a). The change in relative plate motion between South America and Antarctica at 80 Ma caused convergence on this boundary between the South American oceanic lithosphere of the North Weddell Sea, and the Antarctic Peninsula/South Orkney Islands continental crust (Figs. 6e, 8b). As noted by many authors before us (Barker, 2001; Lagabrielle et al., 2009; Vérard et al., 2012; Eagles and Jokat, 2014), this change in relative plate motion caused the initiation of subduction of South American oceanic lithosphere below the Antarctic Peninsula/South Orkney Islands continental crust along the former transform fault (Fig. 8b). Following Ghidella et al. (2002) who called this region the Endurance collision zone, we refer to this as the Endurance subduction zone. Previous authors inferred initiation ages of the Endurance subduction zone varying from 70 to 46 Ma (Barker, 2001; Lagabrielle et al., 2009; Vérard et al., 2012; Eagles and Jokat, 2014). However, the anomalies of the Weddell Sea (Ghidella et al., 2002; Eagles, 2016a; König and Jokat, 2006) reveal that the sharp change in spreading direction from N-S to NW-SE, accommodated by Endurance subduction, already occurred between chrons C34y and C33y, around 80 Ma (Figs. 4; 8a and b).

5.4. Northward propagation of Endurance subduction and delamination of lithospheric mantle

Magnetic anomalies and fracture zones of the Weddell Sea may thus straightforwardly identify the onset of Endurance subduction, but do not explain why subduction also occurred below continental crust originally belonging to South America. In particular, the previously inferred closure of the Rocas Verdes Basin (Barker, 2001; Dalziel et al., 2013) does not offer a straightforward driver for the evolution of the South Sandwich subduction zone: the Rocas Verdes Basin was lost to south-dipping subduction or underthrusting with a suture in Tierra del Fuego (Klepeis et al., 2010). The South Sandwich subduction zone had an initial orientation at high angles to the Rocas Verdes one, had an opposite polarity, and does not logically follow from Rocas Verdes Basin closure. Others assume that the oldest dated arc volcanic rocks dredged from the Scotia Sea floor (~28.5–33 Ma; Barker, 1995; Dalziel et al., 2013) indicate that subduction initiated in the Scotia Sea region around 34 Ma (Crameri et al., 2020; Pearce et al., 2014). Because there is no plate convergence at that time, Pearce et al. (2014) assumed that subduction initiated spontaneously and immediately led to ocean basin formation in the upper plate. But absence of evidence for older arc volcanism from such a scarcely sampled and poorly accessible region does not provide a conclusive argument against older subduction. We therefore explore scenarios that explain the formation of the wide South Sandwich subduction zone by northward, lateral propagation of the Endurance subduction zone. Such propagation should have ruptured South American lithosphere and transferred continental crust of South America into an upper plate position, while the trench propagated

A

85 - 80 Ma: Divergence between South American Plate (SAM) and East Antarctic Plate (EANT) in the future Drake Passage (DP).Transform motion east of South Orkney Islands (SO) continental crust.

B

80 - 71 Ma: Counterclockwise rotation of SAM relative to EANT leads to transform motion between SAM and EANT in the future Drake Passage and Endurance subduction zone (ESZ) initiation below the eastern margin South Orkney Islands

C

71 - 59 Ma: Continued counterclockwise rotation of SAM relative to EANT leads to oblique convergence between SAM and EANT in the future Drake Passage and transform motion at the South America-Antarctica Ridge (SAAR).

D

71 - 59 Ma: Delamination and accretion of part of southern SAM to EANT. Northward propagation of the subduction zone, forming the South Sandwich subduction zone (SSZ). Minimal relative motion in the future Drake Passage and Tierra del Fuego (TdF) region.

E

59 - 50 Ma: After delamination there is minor extension between accreted fragments and SAM.

F

50 - 26 Ma: Start of pre-drift extension and separation of continental fragments from EANT and SAM, leading to initial opening of the Drake Passage (DP) and independent motion of the

G

26 - 6 Ma: Active back-arc spreading in the Scotia Sea separates the Scotia Plate from SAM. Progressive ridge subduction of the SAAR is occurring along the southern segment of the South

H

6 Ma - Present: The South Orkney Microcontinent and Jane Bank (JB) are part of EANT. Tierra del Fuego south of the Magallanes-Fagnano Fault Zone (MFFZ) are part of the Scotia Plate. East Scotia Ridge (ESR) separates the South Sandwich Plate

South American Plate continental crust

South American Plate oceanic crust

East Antarctic Plate continental crust

East Antarctic Plate oceanic crust

Scotia Plate continental crust

Scotia Plate oceanic crust

Continental crust originating from SAM

Continental crust originating from EANT

Fig. 8. Snapshots of the kinematic reconstruction (Antarctica fixed) that serve to highlight the delamination and subsequent accretion of part of South America to the Antarctic Plate. Different plates have different colors, where darker shades represent continental crust and lighter shades represent oceanic crust: Yellow = South American Plate (SAM); Blue = Antarctic Plate and Antarctic Peninsula (AP); Green = Scotia Platea; Gray = (Paleo-)Pacific plates. Horizontal/vertical hatching: Continental crust that originates from the South American/Antarctic Plate; White and black arrows represent absolute plate motion of the South American and Antarctic Plates respectively. Snapshots G and H are at a smaller scale as these encompass a larger area.

northward. Transfer of crustal units from a downgoing to an overriding plate in subduction zones is a common process and typically forms narrow belts of stacked upper crustal nappes that were decoupled from their original mantle and lithospheric underpinnings forming the subducted slab (van Hinsbergen and Schouten, 2021), such as in the Aegean region, Alps, or Himalaya (e.g., Capitanio et al., 2010; Handy et al., 2010; Van Hinsbergen et al., 2005). But the South American crust that transferred to the upper plate of the South Sandwich subduction zone occupied a wide region and there is no evidence that it ever formed a narrow fold-and-thrust belt. Moreover, such accretionary orogens are not associated with lateral propagation of the trench. Perhaps a better analogy is the evolution of the Sula Spur and Banda Sea region in SE Asia (Fig. 9; Spakman and Hall, 2010). There, the Java trench, consuming Australian Plate lithosphere, came into contact with a continental promontory of Australia, the Sula Spur. Australian Plate subduction

continued by propagating into the Australian Plate through delamination of mantle lithosphere from the Sula Spur, leaving the Sula Spur crust as fragments separated by extensional and partly oceanic basins in the upper plate (Fig. 9; see also Spakman and Hall, 2010; their Fig. 3).

We propose that the evolution of the Scotia Sea region has strong parallels with the evolution of the Banda region. This is best explained in a mantle reference frame, for which we take the modern moving hotspot reference frame of Doubrovine et al. (2012). This is possible because we embedded our regional reconstruction within the global framework of plate motion evolution. The Endurance slab had a free edge in the north where it was bounded by a transform (Fig. 8b). A lateral, northward propagation of the Endurance subduction zone to the full width of the South Sandwich subduction zone may occur by delamination of the South American continental lithosphere (Fig. 10), in analogy to the Sula Spur and the invasion of the Java subduction zone into the Banda
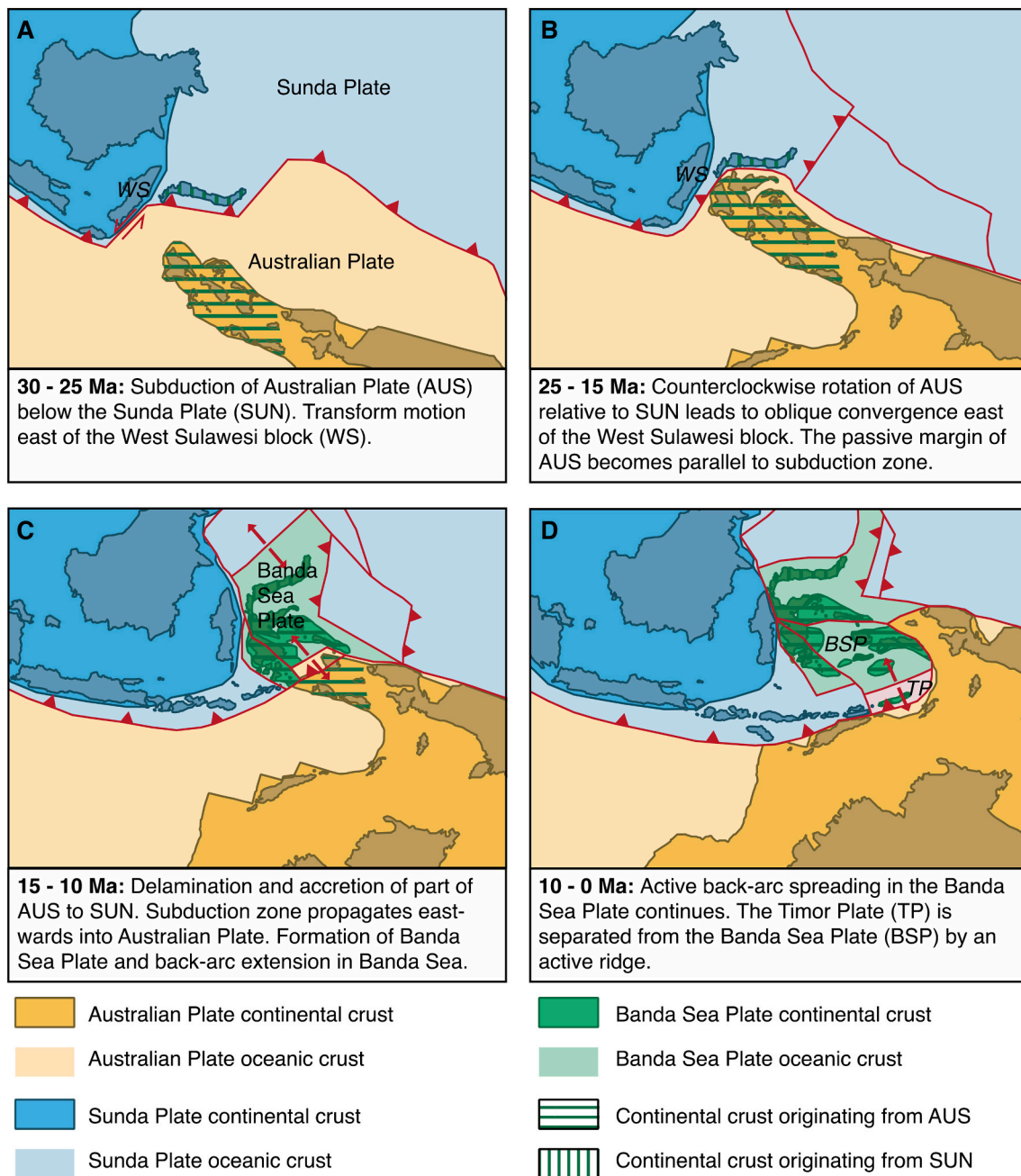
Fig. 9. Snapshots of a kinematic reconstruction showing the subduction of the Australian Plate below the Sunda Plate and the formation of the Banda Sea Plate to illustrate the analogy with the formation of the Scotia Plate. Figures are based on the reconstruction of Hall (2002).
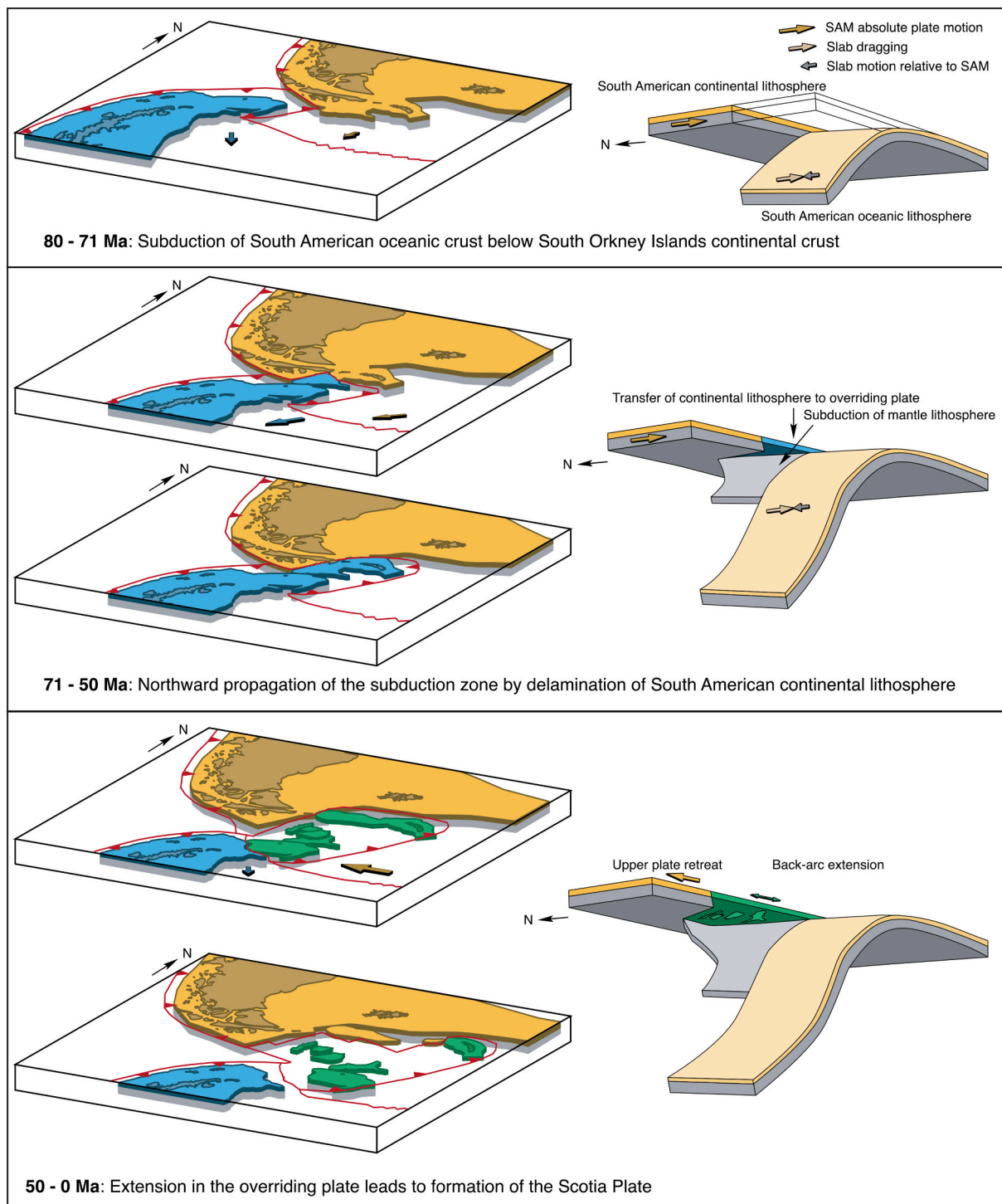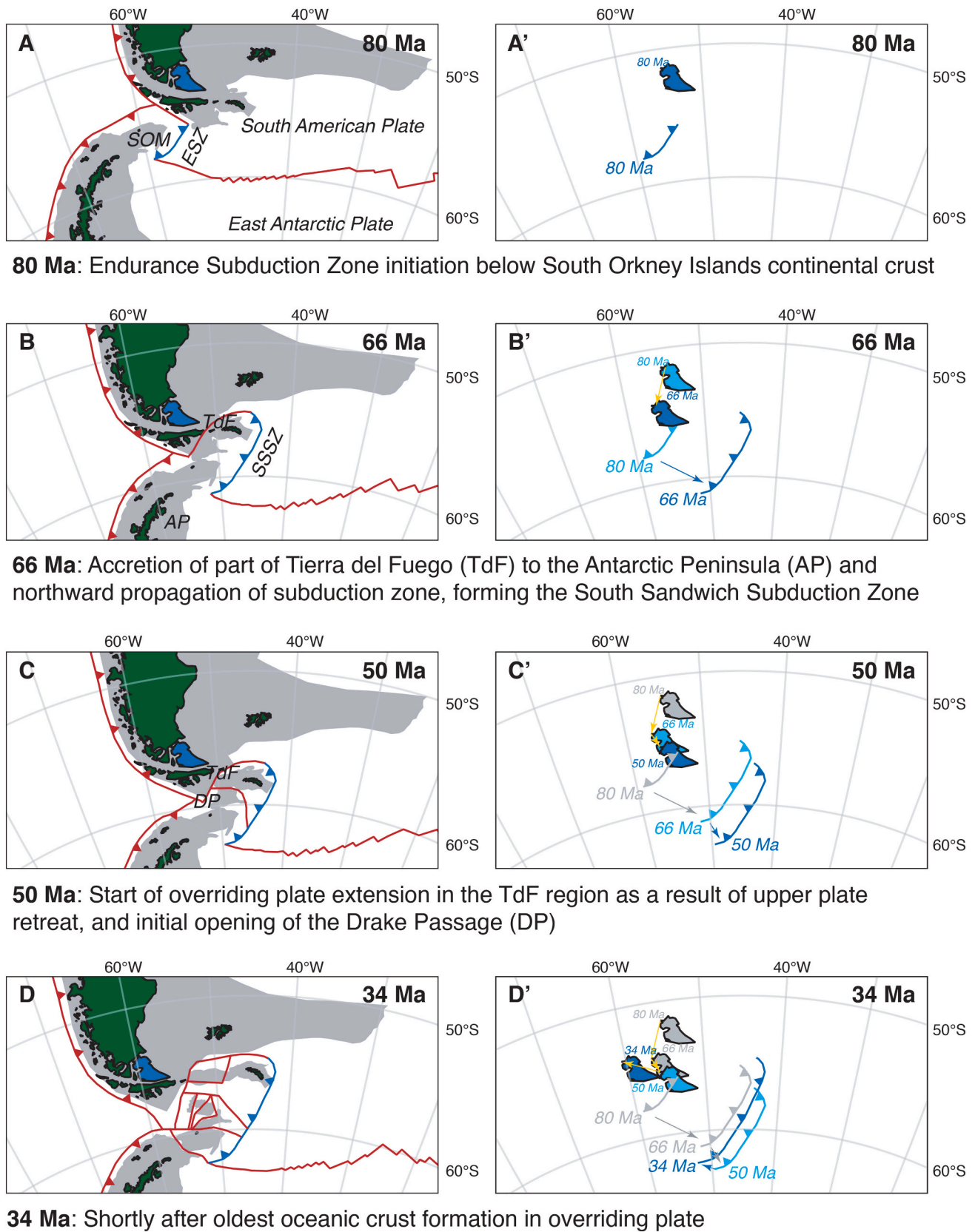
Fig. 10. 3D snapshots of the kinematic reconstruction in a mantle reference frame (see also Fig. 11) and 3D sketches showing the process of delamination and northwards propagation of the Endurance subduction zone and the subsequent transfer of South American continental crust to the overriding plate.

embayment (Fig. 9; Spakman and Hall, 2010).

It is interesting to note that between 70 and 50 Ma, the absolute plate motion direction of South America was southward (Fig. 11; Doubrovine et al., 2012). This means that the northwestward subducting Endurance slab was dragged southward through the mantle by the subducting plate (for slab dragging see Chertova et al., 2014; Spakman et al., 2018; van de Lagemaat et al., 2018). Such slab dragging is resisted by the mantle and leads to northward indentation of South American lithosphere by the slab edge. An analogy of such geodynamic process is the indentation of

the north African margin by the edge of the Gibraltar slab (Spakman et al., 2018). We propound that this indentation may have increased the propensity for the Endurance subduction zone to propagate northward.

Delamination allowed for transfer of the crustal blocks, comprising the future Terror Rise, Bruce Bank, Pirie Bank, Discovery Bank, the North Scotia Ridge and South Georgia microcontinent, to the upper plate (Figs. 8 and 10). The reconstructed South American continental blocks of the Scotia Sea region came close to the Endurance trench from ~71 Ma onwards, and delamination may have started then, but must have

80 Ma: Endurance Subduction Zone initiation below South Orkney Islands continental crust

66 Ma: Accretion of part of Tierra del Fuego (TdF) to the Antarctic Peninsula (AP) and northward propagation of subduction zone, forming the South Sandwich Subduction Zone

50 Ma: Start of overriding plate extension in the TdF region as a result of upper plate retreat, and initial opening of the Drake Passage (DP)

34 Ma: Shortly after oldest oceanic crust formation in overriding plate

Fig. 11. Snapshots of the kinematic reconstruction of the Scotia Sea region since subduction initiation at 80 Ma in a mantle reference frame (Doubrovine et al., 2012). A-H show major plate boundaries, present-day coastlines and continental polygons, while A'-H' show the positions of Isla Grande de Tierra del Fuego and the South Sandwich trench relative to the mantle through time. A'-H' serve to illustrate the respective contributions of overriding plate escape and slab rollback to overriding plate extension through time. The locations of the South Sandwich trench and Isla Grande de Tierra del Fuego that correspond to the snapshot are shown in dark blue, while the location of the previous snapshot is light blue. Earlier locations are in gray.
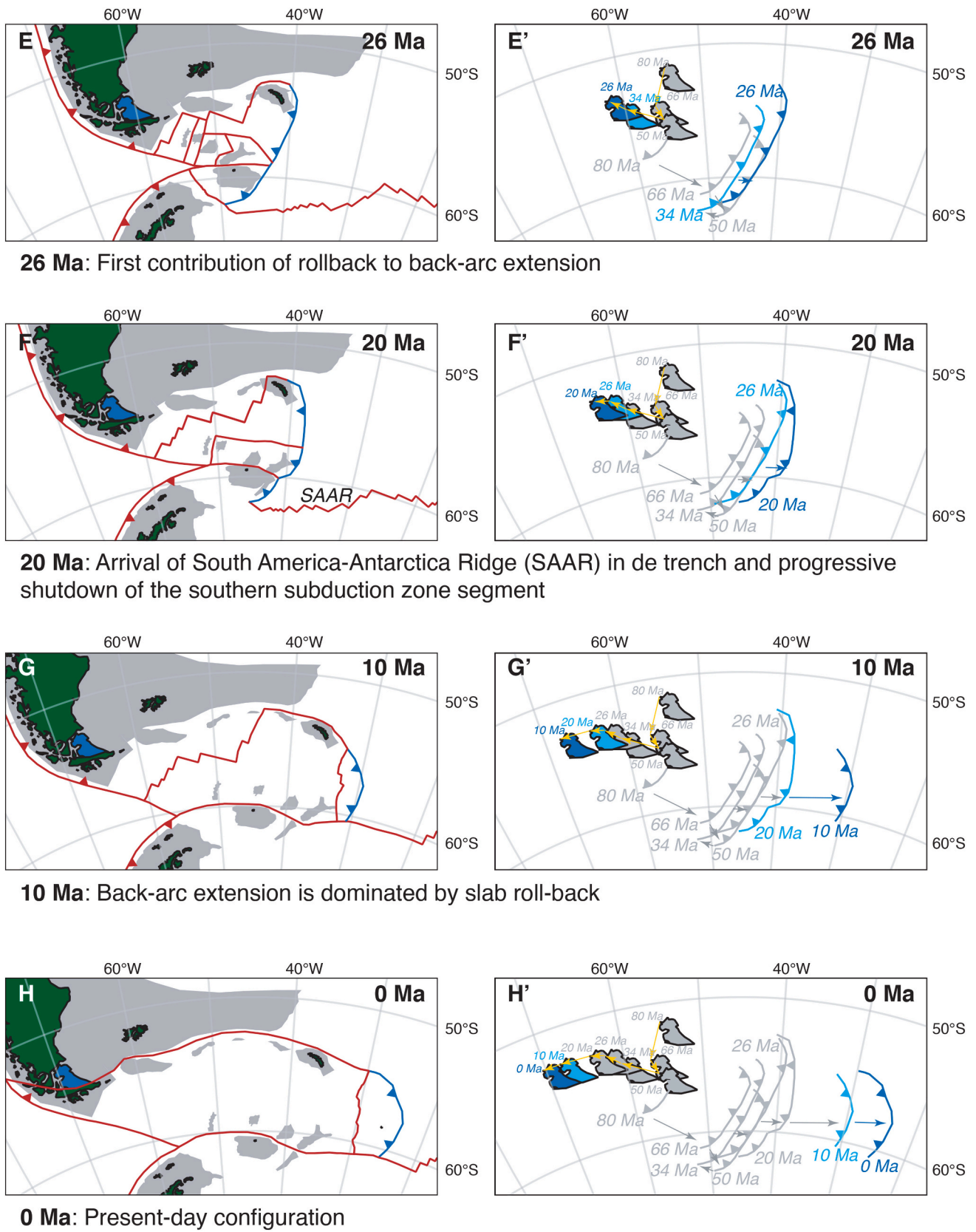
26 Ma: First contribution of rollback to back-arc extension

20 Ma: Arrival of South America-Antarctica Ridge (SAAR) in de trench and progressive shutdown of the southern subduction zone segment

10 Ma: Back-arc extension is dominated by slab roll-back

0 Ma: Present-day configuration

Fig. 11. (*continued*).

been underway by 50 Ma when extension in the Scotia Sea likely started (Fig. 10). In this scenario, it is kinematically feasible that during this northward widening of the subduction zone the Central Scotia Sea

formed between South Georgia and Discovery Bank due to N-S extension (Fig. 6h; see section 5.6).

As a result, post ~50 Ma subduction occurred along the entire width

of the North Weddell Sea oceanic lithosphere, from the ridge with Antarctica to the southern margin of Patagonia (Figs. 6f; 8F, 10). This new trench connected in the north to the transpressional Magallanes fold-and-thrust belt that roughly followed the suture of the Rocas Verdes Basin, and transferred the plate boundary to the trench along the Fuegian Andes.

5.5. Extension in the Scotia Sea

Following formation of the South Sandwich-Endurance subduction system, pre-drift extension in te overriding plate started at 50 Ma (Livermore et al., 2005; Fig. 6g). This caused the South American margin to break up in multiple microplates and the separation of the South Orkney microcontinent and Jane Bank from the Antarctic Peninsula around 40 Ma (Eagles and Livermore, 2002; Figs. 6h, 5i, j). We used the South America-Africa-East Antarctica plate circuit to determine the location of the northern ocean-continent transition conjugate to the southern Weddell Sea margin of Antarctica. This original South American ocean-continent transition was located 150–250 km north of the restored position of the Scotia Sea microcontinents at the onset of oceanic spreading at 36 Ma (Fig. 6h). Such values for pre-drift continental extension are similar to those estimated for passive margins elsewhere (Torsvik et al., 2008). We restored the Scotia Sea microcontinents to the north and west of the reconstructed South American ocean-continent transition (Fig. 6g). We assume a 50 Ma onset for pre-drift extension as widely inferred (Eagles et al., 2006; Livermore et al., 2007; Livermore et al., 2005; Mao and Mohr, 1995).

Following pre-drift extension, oceanic spreading first occurred in the Scan Basin between 35.7 and 29.5 Ma (Schreider et al., 2017; Fig. 6h), followed by the Powell Basin between 29.5 and 21.2 Ma (Eagles and Livermore, 2002). Next, seafloor spreading started in the West Scotia Sea around 26 Ma, in a WNW-ESE direction (Eagles et al., 2005; Fig. 6i). While this spreading ridge remained active, first the Dove Basin opened between 25.3 and 23.3 Ma (Schreider et al., 2018). Around 17.5 Ma, oceanic spreading started in two basins simultaneously, with spreading continuing until 14.2 Ma in the Jane Basin (Bohoyo et al., 2002) and until 13.6 Ma in the Protector Basin (Galindo-Zaldívar et al., 2006; Schreider et al., 2018; Fig. 6j). Finally, spreading started in the East Scotia Basin around 17 Ma and remains active today (Larter et al., 2003; Fig. 6k).

Shortly after formation of anomaly C6 (~19.7 Ma), segments of the South America-Antarctica spreading ridge started to arrive in the South Sandwich subduction zone that bordered the South Scotia Ridge (Fig. 6j). The arrival of the ridge segments in the trench propagated east due to the obliquity of subduction. In absence of net plate convergence, with subduction being balanced by upper plate extension, the arrival of the spreading ridge led to the arrest of subduction, which propagated eastwards along the South Scotia Ridge (Barker et al., 1984). After complete shut-down of the southern segment of the trench, only the ~N-S striking portion of the subduction zone in the east remained, with *E*-W oriented back-arc spreading in the East Scotia Sea (Larter et al., 2003). At 7 Ma, transform motion started in the north, forming the Magallanes-Fagnano Fault Zone, and thereby the Scotia Plate (Torres-Carbonell et al., 2008a; Esteban et al., 2020). Shortly after, seafloor spreading in the West Scotia Basin ceased, at ~6 Ma (Eagles et al., 2005). Subduction continued in the eastern segment of the trench, where South American lithosphere is currently subducting below the South Sandwich Plate, with active E-W back-arc spreading restricted to the East Scotia Basin (Larter et al., 2003; Fig. 6k).

Our reconstructed subduction evolution thus suggests that the Endurance-South Sandwich subduction system involved a single slab during its Late Cretaceous to early Cenozoic evolution. This is consistent with the interpretations of Van der Meer et al. (2018), but we note that the tomography in the Scotia region is of poor resolution. It has been proposed that the eastern part of the slab is related to ongoing South Sandwich subduction, while a more westerly located high velocity zone

represents a fossil part of the slab that formed at an Ancestral South Sandwich subduction zone (Beniest and Schellart, 2020). In this interpretation, the Ancestral South Sandwich subduction zone became inactive in the Miocene after the arrival of the South America-Antarctica Ridge in the southern segment of the trench (Pearce et al., 2014), which led to slab tearing and the onset of oceanic spreading in the East Scotia Basin, separating the South Sandwich arc from the Ancestral South Sandwich arc (Govers and Wortel, 2005; Pearce et al., 2014). The Ancestral South Sandwich subduction zone is the equivalent of our Endurance-South Sandwich subduction zone and these interpretations of the tomography are consistent with our reconstruction.

5.6. Age of the Central Scotia Sea

For the reconstruction of the Central Scotia Sea, with present-day E-W trending magnetic anomalies (Fig. 4; Barker, 1970) two scenarios have previously been proposed. On the one hand, De Wit (1977) suggested that the Central Scotia Sea represents a piece of trapped Mesozoic oceanic crust, as the basin lacks a fossil ridge axis (De Wit, 1977) leading to various scenarios involving a Mesozoic Central Scotia Sea (e.g. Dalziel et al., 2013; Eagles and Jokat, 2014; Pearce et al., 2014). On the other hand, Hill and Barker (1980) speculated an Oligocene-Miocene age and many subsequent reconstructions have assumed a Cenozoic Central Scotia Sea opening (e.g. Barker et al., 1991; Carter et al., 2014; Livermore et al., 2007; Nerlich et al., 2013; Vérard et al., 2012). Here we discuss the implication of our reconstruction for both options.

If we assume a Mesozoic age for the Central Scotia Sea, we restore its position with the opening of the West Scotia Sea until 26 Ma, and with the South Georgia microcontinent before that time. In this reconstruction, the orientation of the Central Scotia Sea anomalies become parallel to the Weddell Sea anomalies. In this case the Central Scotia Sea oceanic crust formed part of the overriding plate above the subduction zone that consumed the Rocas Verdes Basin, which means the width of the Rocas Verdes Basin has implications for the age of the Central Scotia Sea. Our preferred Rocas Verdes Basin model predicts that the anomalies of the Central Scotia Sea formed as part of the Weddell Sea spreading system from ~132–125.9 Ma (chrons M7 – M0).

If we assume that the Central Scotia Sea opened in the Cenozoic, it must be younger than the 50 Ma onset of pre-drift extension (Livermore et al., 2007). The E-W trending lineations imply a N-S opening direction of the basin. In this case the Central Scotia Sea accommodates the northward motion of South Georgia from its 50 Ma position south of Burdwood Bank towards the North Scotia Ridge. To avoid overlap with the marine magnetic anomalies of the West Scotia Sea (Eagles et al., 2005), this northward motion must have occurred before 26 Ma. The bulk of the northward motion occurs before opening of the Scan Basin, and we reconstruct the opening of the Central Scotia between 48.5 and 36.9 Ma, corresponding to chrons C22-C17.

Although both a Mesozoic and Cenozoic Central Scotia Sea are feasible within our reconstruction, we prefer a Cenozoic age for the Central Scotia Sea. Delamination of the South American lithosphere is most likely to have occurred along the passive margin at the transition from continental to oceanic crust. In the case of a Mesozoic Central Scotia Sea, however, part of the oceanic crust was trapped, which means delamination occurred intra-ocean. This may have occurred along a transform fault, but we find the passive margin a more likely location. Moreover, the northward motion of South Georgia that is required by the reconstruction and Cenozoic opening of the Central Scotia Sea fits exactly in the gap that forms when South Georgia separates from Discovery Bank. In addition, the extensive data review by Beniest and Schellart (2020) of currently available geological and geophysical data from the Scotia Sea region advocates for a Cenozoic Central Scotia Sea.

6. Discussion

6.1. Causes for the time lag between subduction initiation and back-arc extension

The onset of Scotia Sea extension started around 50 Ma (Livermore et al., 2005), based on subsidence in the Patagonia-Antarctic Peninsula land bridge around 49–47 Ma (Mao and Mohr, 1995), long after initiation of Endurance subduction. Why did it take so long for upper plate extension to start? To find an explanation, we first explore the contributions of the two potential drivers of upper plate extension: roll-back, i. e., the retreat of the subducting slab through the mantle in the direction of the down-going plate; and upper plate retreat, i.e., the absolute motion of the overriding plate away from the trench (Lallemand et al., 2005; Lallemand et al., 2008; Schepers et al., 2017; van Hinsbergen et al., 2015). We investigate this in the mantle reference frame of Doubrovine et al. (2012) (Fig. 11).

In the mantle frame of reference, Scotia Sea extension since 30 Ma has had a greater contribution from eastward slab roll-back than WNW-ward upper plate retreat. Of the total post-30 Ma extension, ~600 km resulted from WNW-ward upper plate retreat, and ~ 1250 km from slab rollback (Fig. 11e, f, g). But between 50 and 30 Ma, the South Sandwich trench is almost mantle-stationary in the mantle reference frame (Fig. 11c, d, e), suggesting that most, if not all, extension was the result of WNW-directed upper plate retreat (Fig. 11c, d, e).

Interestingly, this WNW-ward motion of the South American Plate started around 50 Ma following a period of ~20–30 Ma of south-directed absolute plate motion (Fig. 11). As noted in the previous section, the pre-50 Ma southward absolute motion of South America (Fig. 11) was oblique to the N*E*-SW-striking trench and the NW-dipping Endurance slab, whose southward dragging was resisted by ambient-slab mantle (Fig. 11 a-c). This would have increased the propensity for northward propagation of the subduction zone. We thus infer that the ~50 Ma onset of extension is a reflection of an absolute plate motion change of South America from southward to WNW-ward. Initially, the trench remained almost mantle stationary. This led to pre-drift extension within the delaminated South American crustal blocks (Fig. 10 c-d). The mantle-stationary trench continued until 30–25 Ma, during which the dragging of the subducted slab (extended by then to ~500 km) to the west-northwest was largely compensated by east-southeast rollback. Such interaction between advancing plate motion and rollback has been observed in laboratory experiments (Schellart, 2005).

Finally, accelerating ESE-ward slab roll-back started around 30–25 Ma when spreading ridges had formed across the upper plate (Eagles et al., 2005). This reduced the dynamic coupling between the down-going South Sandwich slab and the escaping South American Plate, which allowed the slab to roll back more freely. The direction of back-arc basin opening can be related to the changes in slab pull that control slab rollback. The oldest back-arc basins open in a WNW-ESE direction, in the same direction as the absolute plate motion of the South American Plate. When segments of the South America-Antarctica Ridge of the Weddell Sea started to arrive in the southern trench, subduction stopped there. As the existing slab lacked a strong connection to the surface, and slab pull was gradually concentrated to the north where the influence of slab-rollback on back-arc basin opening becomes dominant. This led to a change in the direction of overriding plate extension, from WNW-ESE in the West Scotia Sea to E-W in the East Scotia Sea.

Our analysis illustrates that placing a kinematic reconstruction in a mantle reference frame can reveal the slab motions and controlling geodynamic processes that determine the style of regional subduction and basin evolution, previously also shown by e.g., Spakman et al. (2018) and Van de Lagemaat et al. (2018). Relative reconstructions cannot provide such insights in case subduction is involved. Our reconstruction, placed in a mantle frame of reference, indicates that the onset of Scotia Sea extension and the opening of Drake Passage (Section 6.2) relate to the far-field driven absolute plate motion change of the South American Plate. This started to drive South America WNW-ward relative to the mantle around 50 Ma (Fig. 11) while the slab assumed a near-stationary position in the mantle for a 20–25 Ma period. Slab roll-back, which was previously inferred to be the sole driver of Drake Passage opening in the Eocene, probably did not start until 30–25 Ma when slab pull started to dominate the forcing of subduction in concert with back-arc basin opening (Fig. 11).

6.2. Opening of the Drake Passage and onset of circumpolar ocean flow in a global plate kinematic context

The opening of the Drake Passage occurred after the 50 Ma onset of overriding plate extension in a time interval of global geodynamic and climatic change. The onset of westward absolute South American Plate motion that is thought to have driven the rise of the Andes (Faccenna et al., 2017; Schellart, 2017) occurred in a time of global plate reorganization that also affected the Indian, Australian, and Pacific Plates (Müller et al., 2016; Torsvik et al., 2017; Vaes et al., 2019; Whittaker et al., 2007). It also coincides with first throughflow of ocean water through the Tasmanian Gateway between Australia and Antarctica (Bijl et al., 2013). Long-term global cooling started around the same time (Cramwinckel et al., 2018) and is thought to be related to global atmospheric CO_2 decline through enhanced weathering, stimulated by enhanced silicate rock exposure from uplift of the Himalaya and Andes (Kump et al., 2000). This study shows that the same major plate reorganization responsible for the mid-Eocene tectonic development of climate-cooling mountain ranges also initiated the opening of the Drake Passage, clearing a major barrier for circumpolar flow of ocean water (a proto-Antarctic Circumpolar Current (ACC); e.g., Hill et al., 2013; Houben et al., 2019). Independent of CO_2 decline, this paleogeographic change promoted further regional cooling of Antarctica (Sijp et al., 2014), which preconditioned Antarctica for glaciation. This study thus demonstrates the influence of geodynamic changes in critical areas on the sensitivity of Antarctic climate and cryosphere to radiative forcing in the Cenozoic. Our reconstruction shows that a deep oceanic connection between the Pacific and the Atlantic started sometime between 50 and 36 Ma, in line with the 41 Ma onset of deep-water throughflow through the Drake Passage shown in geochemical records (Scher and Martin, 2006). However, it also shows this ocean connection was not unique: Cretaceous deep-water connections may have existed, and connections may have closed post-41 Ma as well. Ocean connections remained strongly constricted until <26 Ma, by obstruction through continental blocks and narrow deep-ocean passageways. This agrees with interpretations of a weak ACC and relatively flat latitudinal sea surface temperature gradients across the Southern Ocean during the Oligocene (Bijl et al., 2018; Evangelinos et al., 2020; Hartman et al., 2018; Sala-barnada et al., 2018), which continued into the Miocene (~10 Ma; Sangiorgi et al., 2018). Although this may not be all due to the development of the Scotia Sea and other factors may have contributed (climate deterioration and ice sheet expansion), the Drake Passage was strongly constricted for most of the late Paleogene-early Neogene, and strengthening of the ACC coincides with major tectonic widening of the Scotia Sea (Fig. 10g; see also Supplementary Fig. 1).

7. Conclusions

Here we present a new kinematic reconstruction of the Scotia Sea region since the Early Jurassic (182 Ma). The aim of this study was to assess when and why subduction initiated that led to the formation of the South Sandwich subduction zone, and to explain the overriding plate position of both the Antarctic and South American plates. Our reconstruction results from systematic integration of available quantitative kinematic constraints, derived from marine geophysical, geological and paleomagnetic data, and the implementation of a global plate circuit, and enables the following conclusions:

1) The present-day South Sandwich subduction zone has its origin in the formation of a Late Cretaceous (~80 Ma) subduction zone below South Orkney Islands continental crust: the Endurance subduction zone. The occurrence of convergence along the South Orkney continental margin follows from the South American-Africa-Antarctica plate circuit and marine magnetic anomalies and fracture zones in the Weddell Sea. We suggest that delamination of the South American continental lithosphere led to the northward propagation of the Endurance subduction zone to form the South Sandwich subduction zone. Delamination allowed for transfer of part of South American continental crust to the upper plate. Delamination was underway by 50 Ma when extension in the Scotia Sea started, but may have started around 71 Ma, when the South American continental margin came close to the Endurance trench.

2) Our kinematic reconstruction predicts that the Rocas Verdes Basin was up to 250 km wide. Cretaceous (~113–102 Ma) closure of the basin was accompanied by 25° counter-clockwise rotation of its southwestern margin. Excess rotations within Tierra del Fuego are ascribed to local block rotations related to post 7 Ma left-lateral strike slip motion of the Magallanes-Fagnano Fault Zone.

3) Overriding plate extension and subsequent opening of the Drake Passage started at 50 Ma. The time lag between subduction initiation and overriding plate extension is explained by the absolute plate motions of South America and Antarctica. Between Late Cretaceous subduction initiation and 50 Ma the absolute plate motion of South America was to the south, dragging the Endurance subduction system southward, and not contributing to lithosphere subduction. Around 50 Ma, the absolute plate motion of South America changed to west-northwest. The length of the slab was sufficient to provide a temporal balance between advancing motion and rollback, which led to the onset of upper plate extension as a result of motion of South America away from the trench. Our analysis thus suggests that early extension in the Scotia Sea region was the result of far-field changes in absolute plate motions.

4) The formation of oceanic spreading centres in the Scotia Sea around 35–25 Ma reduced the dynamic coupling between the down-going slab and escaping overriding plate, allowing the slab to roll-back freely. Subsequently, overriding plate extension resulted from both upper plate retreat and slab roll-back, dominated by the latter mechanism. The direction of back-arc basin opening is related to the relative influence of upper plate retreat and slab rollback. These inferences of slab evolution can only be made when using a mantle frame of reference, which our global circuit approach allows.

5) We deduce that the closely spaced micro-continental blocks in the Drake Passage Region must have initially limited throughflow of the Antarctic Circumpolar Current. Strengthening of the Antarctic Circumpolar Current in the Miocene coincides with major tectonic widening of the Scotia Sea.

Declaration of Competing Interest

The authors declare that they have no known competing financial interests or personal relationships that could have appeared to influence the work reported in this paper.

Acknowledgements

Appendix B. Supplementary data

1) The data files of the GPlates reconstruction of the Scotia Sea region: a rotation (.rot) file, a GPlates shapefile (.gpml) containing polygons, and a GPlates shapefile (.gpml) of the isochrons based on marine magnetic anomaly lineations; 2) The paleomagnetic data compilation: an excel file of the paleomagnetic data and two .pub files of the data that can be loaded into Paleomagnetism.org (Koymans et al., 2020); Supplementary data to this article can be found online at [https://doi.org/10.1016/j.earscirev.2021.103551].

References

Alvarez-Marrón, J., McClay, K., Harambour, S., Rojas, L., Skarmeta, J., 1993. Geometry and evolution of the frontal part of the Magallanes foreland thrust and fold belt (Vicuña Area), Tierra del Fuego, Southern Chile. AAPG Bull. 77 (11), 1904–1921.

Auzemery, A., Willingshofer, E., Yamato, P., Duretz, T., Sokoutis, D., 2020. Strain localization mechanisms for subduction initiation at passive margins. Glob. Planet. Chang. 103323.

Bakhmutov, V., Shpyra, V., 2011. Palaeomagnetism of late Cretaceous-Paleocene igneous rocks from the western part of the Antarctic Peninsula (argentine Islands Archipelago). Geol. Q. 55 (4), 285–300.

Barker, P.F., 1970. Plate tectonics of the Scotia Sea region. Nature 228 (5278), 1293–1296.

Barker, P.F., 1995. Tectonic Framework of the East Scotia Sea, Backarc Basins. Springer, pp. 281–314.

Barker, P.F., 2001. Scotia Sea regional tectonic evolution: implications for mantle flow and palaeocirculation. Earth Sci. Rev. 55 (1–2), 1–39.

Barker, P., Jahn, R., 1980. A marine geophysical reconnaissance of the Weddell Sea. Geophys. J. Int. 63 (1), 271–283.

Barker, P.F., Lawver, L.A., 1988. South American-Antarctic plate motion over the past 50 Myr, and the evolution of the South American-Antarctic ridge. Geophys. J. Int. 94 (3), 377–386.

Barker, P.F., Hill, I., Weaver, S., Pankhurst, R., 1982. The Origin of the Eastern South Scotia Ridge as an Intraoceanic Island Arc.

Barker, P.F., Barber, P.L., King, E.C., 1984. An early Miocene ridge crest-trench collision on the South Scotia Ridge near 36 W. Tectonophysics 102 (1–4), 315–332.

Barker, P.F., Dalziel, I.y., Storey, B., 1991. Tectonic development of the Scotia Arc region. Geol. Antarct. 215–248.

Beniest, A., Schellart, W.P., 2020. A geological map of the Scotia Sea area constrained by bathymetry, geological data, geophysical data and seismic tomography models from the deep mantle. Earth Sci. Rev. 103391.

Bernard, A., Munschy, M., Rotstein, Y., Sauter, D., 2005. Refined spreading history at the Southwest Indian Ridge for the last 96 Ma, with the aid of satellite gravity data. Geophys. J. Int. 162 (3), 765–778.

Betka, P.M., 2013. Structure of the Patagonian Fold-Thrust Belt in the Magallanes Region of Chile, 53°-55° S Lat.

Betka, P., Klepeis, K., Mosher, S., 2015. Along-strike variation in crustal shortening and kinematic evolution of the base of a retroarc fold-and-thrust belt: Magallanes, Chile 53° S–54° S. GSA Bull. 127 (7–8), 1108–1134.

Betka, P., Klepeis, K., Mosher, S., 2016. Fault kinematics of the Magallanes-Fagnano fault system, southern Chile; an example of diffuse strain and sinistral transtension along a continental transform margin. J. Struct. Geol. 85, 130–153.

Biddle, K., Uliana, M., Mitchum Jr., R., Fitzgerald, M., Wright, R., 1986. The stratigraphic and structural evolution of the central and eastern Magallanes Basin, southern South America. Foreland Basins 41–61.

Bijl, P.K., Bendle, J.A., Bohaty, S.M., Pross, J., Schouten, S., Tauxe, L., Stickley, C.E., McKay, R.M., Röhl, U., Olney, M., 2013. Eocene cooling linked to early flow across the Tasmanian Gateway. Proc. Natl. Acad. Sci. 110 (24), 9645–9650.

Bijl, P.K., Houben, A.J., Hartman, J.D., Pross, J., Salabarnada, A., Escutia, C., Sangiorgi, F., 2018. Paleoceanography and ice sheet variability offshore Wilkes Land, Antarctica-Part 2: Insights from Oligocene-Miocene dinoflagellate cyst assemblages. Clim. Past 14 (7), 1015–1033.

Bingham, R.G., Ferraccioli, F., King, E.C., Larter, R.D., Pritchard, H.D., Smith, A.M., Vaughan, D.G., 2012. Inland thinning of West Antarctic Ice Sheet steered along subglacial rifts. Nature 487 (7408), 468–471.

Bohoyo, F., Galindo-Zaldívar, J., Maldonado, A., Schreider, A., Suriñach, E., 2002. Basin development subsequent to ridge-trench collision: the Jane Basin, Antarctica. Mar. Geophys. Res. 23 (5–6), 413–421.

Boschman, L.M., van Hinsbergen, D.J., Torsvik, T.H., Spakman, W., Pindell, J.L., 2014. Kinematic reconstruction of the Caribbean region since the early Jurassic. Earth Sci. Rev. 138, 102–136.

Boyden, J.A., Müller, R.D., Gurnis, M., Torsvik, T.H., Clark, J.A., Turner, M., Ivey-Law, H., Watson, R.J., Cannon, J.S., 2011. Next-generation plate-tectonic reconstructions using GPlates. In: Geoinformatics: Cyberinfrastructure for the Solid Earth Sciences. Cambridge University Press, Cambridge, pp. 95–113. ISBN 9780521897150.

Burns, K., Rickard, M., Belbin, L., Chamalaun, F., 1980. Further palaeomagnetic confirmation of the Magellanes orocline. Tectonophysics 63 (1–4), 75–90.

Burton-Johnson, A., Riley, T., 2015. Autochthonous v. accreted terrane development of continental margins: a revised in situ tectonic history of the Antarctic Peninsula. J. Geol. Soc. 172 (6), 822–835.

Butterworth, P., Crame, J., Howlett, P., Macdonald, D., 1988. Lithostratigraphy of Upper Jurassic-lower cretaceous strata of eastern Alexander Island, Antarctica. Cretac. Res. 9 (3), 249–264.

Calderón, M., Fildani, A., Herve, F., Fanning, C., Weislogel, A., Cordani, U., 2007. Late Jurassic bimodal magmatism in the northern sea-floor remnant of the Rocas Verdes basin, southern Patagonian Andes. J. Geol. Soc. 164 (5), 1011–1022.

Cande, S.C., Stock, J.M., Müller, R.D., Ishihara, T., 2000. Cenozoic motion between east and West Antarctica. Nature 404 (6774), 145–150.

Cande, S.C., Patriat, P., Dyment, J., 2010. Motion between the Indian, Antarctic and African plates in the early Cenozoic. Geophys. J. Int. 183 (1), 127–149.

Capitanio, F., Morra, G., Goes, S., Weinberg, R., Moresi, L., 2010. India–Asia convergence driven by the subduction of the Greater Indian continent. Nat. Geosci. 3 (2), 136–139.

Carey, S.W., 1955. The Orocline Concept in Geotectonics-Part I, Papers and Proceedings of the Royal Society of Tasmania, pp. 255–288.

Carter, A., Curtis, M., Schwanethal, J., 2014. Cenozoic tectonic history of the South Georgia microcontinent and potential as a barrier to Pacific-Atlantic through flow. Geology 42 (4), 299–302.

Chertova, M., Spakman, W., Geenen, T., Van Den Berg, A., Van Hinsbergen, D., 2014. Underpinning tectonic reconstructions of the western Mediterranean region with dynamic slab evolution from 3-D numerical modeling. J. Geophys. Res. Solid Earth 119 (7), 5876–5902.

Civile, D., Lodolo, E., Vuan, A., Loreto, M., 2012. Tectonics of the Scotia–Antarctica plate boundary constrained from seismic and seismological data. Tectonophysics 550, 17–34.

Crameri, F., Magni, V., Domeier, M., Shephard, G.E., Chotalia, K., Cooper, G., Eakin, C. M., Grima, A.G., Gürer, D., Király, Á., 2020. A transdisciplinary and community-driven database to unravel subduction zone initiation. Nat. Commun. 11 (1), 1–14.

Cramwinckel, M.J., Huber, M., Kocken, I.J., Agnini, C., Bijl, P.K., Bohaty, S.M., Frieling, J., Goldner, A., Hilgen, F.J., Kip, E.L., 2018. Synchronous tropical and polar temperature evolution in the Eocene. Nature 559 (7714), 382–386.

Cunningham, W.D., 1993. Strike-slip faults in the southernmost Andes and the development of the Patagonian orocline. Tectonics 12 (1), 169–186.

Cunningham, W., 1994. Uplifted ophiolitic rocks on Isla Gordon, southernmost Chile: implications for the closure history of the Rocas Verdes marginal basin and the tectonic evolution of the Beagle Channel region. J. S. Am. Earth Sci. 7 (2), 135–147.

Cunningham, W.D., 1995. Orogenesis at the southern tip of the Americas: the structural evolution of the Cordillera Darwin metamorphic complex, southernmost Chile. Tectonophysics 244 (4), 197–229.

Cunningham, W.D., Klepeis, K.A., Gose, W.A., Dalziel, I.W., 1991. The Patagonian Orocline: New paleomagnetic data from the Andean magmatic arc in Tierra del Fuego, Chile. J. Geophys. Res. Solid Earth 96 (B10), 16061–16067.

Dalziel, I., 1981. Back-arc extension in the southern Andes: a review and critical reappraisal. Philos. Trans. Royal Soc. Lond. Ser. A Math. Phys. Sci. 300 (1454), 319–335.

Dalziel, I., 1986. Collision and Cordilleran orogenesis: an Andean perspective. Geol. Soc. Lond., Spec. Publ. 19 (1), 389–404.

Dalziel, I., 2006. On the extent of the active West Antarctic rift system. In: Terra Antartica Reports, 12, pp. 193–202.

Dalziel, I.W., Elliot, D.H., 1982. West Antarctica: problem child of Gondwanaland. Tectonics 1 (1), 3–19.

Dalziel, I.W., de Wit, M.J., Palmer, K.F., 1974. Fossil marginal basin in the southern Andes. Natur 250 (5464), 291–294.

Dalziel, I., Dott Jr., R., Winn Jr., R., Bruhn, R., 1975. Tectonic relations of South Georgia Island to the southernmost Andes. Geol. Soc. Am. Bull. 86 (7), 1034–1040.

Dalziel, I.W., Lawver, L., Murphy, J., 2000. Plumes, orogenesis, and supercontinental fragmentation. Earth Planet. Sci. Lett. 178 (1–2), 1–11.

Dalziel, I.W., Lawver, L.A., Norton, I.O., Gahagan, L.M., 2013. The Scotia Arc: genesis, evolution, global significance. Annu. Rev. Earth Planet. Sci. 41.

De Wit, M.J., 1977. The evolution of the Scotia Arc as a key to the reconstruction of southwestern Gondwanaland. Tectonophysics 37 (1–3), 53–81.

de Wit, M.J., Stern, C.R., 1981. Variations in the degree of crustal extension during formation of a back-arc basin. Tectonophysics 72 (3–4), 229–260.

Deenen, M.H., Langereis, C.G., van Hinsbergen, D.J., Biggin, A.J., 2011. Geomagnetic secular variation and the statistics of palaeomagnetic directions. Geophys. J. Int. 186 (2), 509–520.

DeMets, C., Gordon, R.G., Argus, D.F., 2010. Geologically current plate motions. Geophys. J. Int. 181 (1), 1–80.

Dott, R., Winn, R., Dewit, M., Bruhn, R., 1977. Tectonic and sedimentary significance of cretaceous Tekenika Beds of Tierra del Fuego. Nature 266 (5603), 620–622.

Doubleday, P., Macdonald, D., Nell, P., 1993. Sedimentology and structure of the trench-slope to forearc basin transition in the Mesozoic of Alexander Island, Antarctica. Geol. Mag. 130 (6), 737–754.

Doubrovine, P.V., Steinberger, B., Torsvik, T.H., 2012. Absolute plate motions in a reference frame defined by moving hot spots in the Pacific, Atlantic, and Indian oceans. J. Geophys. Res. Solid Earth 117 (B9).

Eagles, G., 2010. The age and origin of the central Scotia sea. Geophys. J. Int. 183 (2), 587–600.

Eagles, G., 2016a. Plate kinematics of the Rocas Verdes Basin and Patagonian orocline. Gondwana Res. 37, 98–109.

Eagles, G., 2016b. Tectonic reconstructions of the Southernmost Andes and the Scotia Sea during the opening of the Drake Passage. In: Geodynamic Evolution of the Southernmost Andes. Springer, pp. 75–108.

Eagles, G., Jokat, W., 2014. Tectonic reconstructions for paleobathymetry in Drake Passage. Tectonophysics 611, 28–50.

Eagles, G., Livermore, R.A., 2002. Opening history of Powell Basin, Antarctic Peninsula. Mar. Geol. 185 (3–4), 195–205.

Eagles, G., Livermore, R.A., Fairhead, J.D., Morris, P., 2005. Tectonic evolution of the west Scotia Sea. J. Geophys. Res. Solid Earth 110 (B2).

Eagles, G., Livermore, R., Morris, P., 2006. Small basins in the Scotia Sea: the Eocene Drake passage gateway. Earth Planet. Sci. Lett. 242 (3–4), 343–353.

Eagles, G., Larter, R.D., Gohl, K., Vaughan, A.P., 2009. West Antarctic rift system in the Antarctic Peninsula. Geophys. Res. Lett. 36 (21).

Esteban, F.D., Ormazabal, J.P., Palma, F., Cayo, L.E., Lodolo, E., Tassone, A., 2020. Strike-slip related folding within the Malvinas/Falkland Trough (South-Western Atlantic Ocean). J. S. Am. Earth Sci. 98, 102452.

Evangelinos, D., Escutia, C., Etourneau, J., Hoem, F., Bijl, P., Boterblom, W., van de Flierdt, T., Valero, L., Flores, J.-A., Rodriguez-Tovar, F.J., 2020. Late oligocene-miocene proto-antarctic circumpolar current dynamics off the Wilkes Land margin, East Antarctica. Glob. Planet. Chang. 103221.

Ewing, J., Ludwig, W., Ewing, M., Eittreim, S., 1971. Structure of the Scotia Sea and Falkland plateau. J. Geophys. Res. 76 (29), 7118–7137.

Faccenna, C., Oncken, O., Holt, A.F., Becker, T.W., 2017. Initiation of the Andean orogeny by lower mantle subduction. Earth Planet. Sci. Lett. 463, 189–201.

Fildani, A., Cope, T.D., Graham, S.A., Wooden, J.L., 2003. Initiation of the Magallanes foreland basin: timing of the southernmost Patagonian Andes orogeny revised by detrital zircon provenance analysis. Geology 31 (12), 1081–1084.

Fisher, R., 1953. Dispersion on a Sphere: Proceedings of the Royal Society London, 217.

Fitzgerald, P., Baldwin, S., 1997. Detachment fault model for the evolution of the Ross Embayment. In: The Antarctic Region: Geological Evolution and Processes, pp. 555–564.

Fitzsimons, I., 2000. Grenville-age basement provinces in East Antarctica: evidence for three separate collisional orogens. Geology 28 (10), 879–882.

Fosdick, J.C., Romans, B.W., Fildani, A., Bernhardt, A., Calderón, M., Graham, S.A., 2011. Kinematic evolution of the Patagonian retroarc fold-and-thrust belt and Magallanes foreland basin, Chile and Argentina, 51 30′ S. Bulletin 123 (9–10), 1679–1698.

Fosdick, J.C., Grove, M., Hourigan, J.K., Calderon, M., 2013. Retroarc deformation and exhumation near the end of the Andes, southern Patagonia. Earth Planet. Sci. Lett. 361, 504–517.

Gaina, C., Torsvik, T.H., van Hinsbergen, D.J., Medvedev, S., Werner, S.C., Labails, C., 2013. The African Plate: a history of oceanic crust accretion and subduction since the Jurassic. Tectonophysics 604, 4–25.

Galindo-Zaldívar, J., Bohoyo, F., Maldonado, A., Schreider, A., Surinach, E., Vázquez, J. T., 2006. Propagating rift during the opening of a small oceanic basin: the Protector Basin (Scotia Arc, Antarctica). Earth Planet. Sci. Lett. 241 (3–4), 398–412.

Galindo-Zaldívar, J., Puga, E., Bohoyo, F., González, F.J., Maldonado, A., Martos, Y.M., Pérez, L.F., Ruano, P., Schreider, A.A., Somoza, L., 2014. Reprint of "Magmatism, structure and age of dove Basin (Antarctica): a key to understanding South Scotia Arc development". Glob. Planet. Chang. 123, 249–268.

Gao, L., Zhao, Y., Yang, Z., Liu, J., Liu, X., Zhang, S.H., Pei, J., 2018. New paleomagnetic and 40Ar/39Ar geochronological results for the South Shetland Islands, West Antarctica, and their tectonic implications. J. Geophys. Res. Solid Earth 123 (1), 4–30.

Ghidella, M.E., Yáñez, G., LaBrecque, J.L., 2002. Revised tectonic implications for the magnetic anomalies of the western Weddell Sea. Tectonophysics 347 (1–3), 65–86.

Ghiglione, M.C., Ramos, V.A., 2005. Progression of deformation and sedimentation in the southernmost Andes. Tectonophysics 405 (1–4), 25–46.

Ghiglione, M.C., Suarez, F., Ambrosio, A., Da Poian, G., Cristallini, E.O., Pizzio, M.F., Reinoso, R.M., 2009. Structure and evolution of the Austral Basin fold-thrust belt, southern Patagonian Andes. Rev. Asoc. Geol. Argent. 65 (1), 215–226.

Ghiglione, M.C., Quinteros, J., Yagupsky, D., Bonillo-Martínez, P., Hlebszevtich, J., Ramos, V.A., Vergani, G., Figueroa, D., Quesada, S., 2010. Structure and tectonic history of the foreland basins of southernmost South America. J. S. Am. Earth Sci. 29 (2), 262–277.

Ghiglione, M.C., Likerman, J., Barberón, V., Giambiagi, L.B., Aguirre-Urreta, B., Suarez, F., 2014. Geodynamic context for the deposition of coarse-grained deep-water axial channel systems in the Patagonian Andes. Basin Res. 26 (6), 726–745.

Gohl, K., Teterin, D., Eagles, G., Netzeband, G., Grobys, J., Parsiegla, N., Schlüter, P., Leinweber, V.T., Larter, R.D., Uenzelmann-Neben, G., 2007. Geophysical survey reveals tectonic structures in the Amundsen Sea embayment, West Antarctica. In: US Geological Survey Open-File Report, 2007–1047 (http://pubs.usgs.gov/of/2007/1047/srp/srp047/).

González, V.R., Puigdomenech, C.G., Zaffarana, C.B., Vizán, H., Somoza, R., 2020. Paleomagnetic evidence of the brittle deformation of the Central Patagonian Batholith at Gastre area (Chubut Province, Argentina). J. S. Am. Earth Sci. 98, 102442.

Goodge, J.W., 2020. Geological and tectonic evolution of the Transantarctic Mountains, from ancient craton to recent enigma. Gondwana Res. 80, 50–122.

Govers, R., Wortel, M., 2005. Lithosphere tearing at STEP faults: Response to edges of subduction zones. Earth Planet. Sci. Lett. 236 (1–2), 505–523.

Gradstein, F.M., Ogg, J.G., Schmitz, M.B., Ogg, G.M., 2012. The Geologic Time Scale 2012. Elsevier.

Granot, R., Dyment, J., 2018. Late Cenozoic unification of East and West Antarctica. Nat. Commun. 9 (1), 1–10.

Granot, R., Cande, S., Stock, J., Damaske, D., 2013. Revised Eocene-Oligocene kinematics for the West Antarctic rift system. Geophys. Res. Lett. 40 (2), 279–284.

Grunow, A., 1993. New paleomagnetic data from the Antarctic Peninsula and their tectonic implications. J. Geophys. Res. Solid Earth 98 (B8), 13815–13833.

Guillot, M.G., 2016. Magmatic evolution of the southernmost Andes and its relation with subduction processes. In: Geodynamic Evolution of the Southernmost Andes. Springer, pp. 37–74.

Gurnis, M., Hall, C., Lavier, L., 2004. Evolving force balance during incipient subduction. Geochem. Geophys. Geosyst. 5 (7).

Hall, R., 2002. Cenozoic geological and plate tectonic evolution of SE Asia and the SW Pacific: computer-based reconstructions, model and animations. Journal of Asian Earth Sciences 20 (4), 353–431.

Handy, M.R., Schmid, S.M., Bousquet, R., Kissling, E., Bernoulli, D., 2010. Reconciling plate-tectonic reconstructions of Alpine Tethys with the geological–geophysical record of spreading and subduction in the Alps. Earth Sci. Rev. 102 (3–4), 121–158.

Harley, S., 2003. Archaean-Cambrian crustal development of East Antarctica: metamorphic characteristics and tectonic implications. Geol. Soc. Lond., Spec. Publ. 206 (1), 203–230.

Hartman, J.D., Sangiorgi, F., Escutia Dotti, C., 2018. Paleoceanography and Ice Sheet Variability Offshore Wilkes Land, Antarctica–Part 3: Insights from Oligocene–Miocene TEX86-Based Sea Surface Temperature Reconstructions.

Hathway, B., 2000. Continental rift to back-arc basin: Jurassic–cretaceous stratigraphical and structural evolution of the Larsen Basin, Antarctic Peninsula. J. Geol. Soc. 157 (2), 417–432.

Heine, C., Zoethout, J., Müller, R.D., 2013. Kinematics of the South Atlantic rift. Solid Earth 4 (2), 215–253.

Hervé, M., Suárez, M., Puig, A., 1984. The Patagonian Batholith S of Tierra del Fuego, Chile: timing and tectonic implications. J. Geol. Soc. 141 (5), 909–917.

Herve, F., Pankhurst, R.J., Fanning, C., Calderón, M., Yaxley, G., 2007. The south Patagonian batholith: 150 my of granite magmatism on a plate margin. Lithos 97 (3–4), 373–394.

Hill, I.A., Barker, P.F., 1980. Evidence for Miocene back-arc spreading in the central Scotia Sea. Geophys. J. Int. 63 (2), 427–440.

Hill, D.J., Haywood, A.M., Valdes, P.J., Francis, J.E., Lunt, D.J., Wade, B.S., Bowman, V. C., 2013. Paleogeographic controls on the onset of the Antarctic circumpolar current. Geophys. Res. Lett. 40 (19), 5199–5204.

Holt, J.W., Blankenship, D.D., Morse, D.L., Young, D.A., Peters, M.E., Kempf, S.D., Richter, T.G., Vaughan, D.G., Corr, H.F., 2006. New boundary conditions for the West Antarctic Ice Sheet: Subglacial topography of the Thwaites and Smith glacier catchments. Geophys. Res. Lett. 33 (9).

Houben, A.J., Bijl, P.K., Sluijs, A., Schouten, S., Brinkhuis, H., 2019. Late Eocene Southern Ocean cooling and invigoration of circulation preconditioned Antarctica for full-scale glaciation. Geochem. Geophys. Geosyst. 20 (5), 2214–2234.

Jokat, W., Boebel, T., König, M., Meyer, U., 2003. Timing and geometry of early Gondwana breakup. J. Geophys. Res. Solid Earth 108 (B9).

Jones, P.C., Johnson, A.C., von Frese, R.R., Corr, H., 2002. Detecting rift basins in the Evans Ice Stream region of West Antarctica using airborne gravity data. Tectonophysics 347 (1–3), 25–41.

Jordan, T., Ferraccioli, F., Vaughan, D., Holt, J., Corr, H., Blankenship, D., Diehl, T., 2010. Aerogravity evidence for major crustal thinning under the Pine Island Glacier region (West Antarctica). Bulletin 122 (5–6), 714–726.

Jordan, T.A., Riley, T.R., Siddoway, C.S., 2020. The geological history and evolution of West Antarctica. Nat. Rev. Earth Environ. 1–17.

King, R., 1955. The remanent magnetism of artificially deposited sediments. Geophys. Suppl. Mon. Not. Royal Astron. Soc. 7 (3), 115–134.

Klepeis, K.A., 1994a. The Magallanes and Deseado fault zones: Major segments of the South American-Scotia transform plate boundary in southernmost South America, Tierra del Fuego. J. Geophys. Res. Solid Earth 99 (B11), 22001–22014.

Klepeis, K.A., 1994b. Relationship between uplift of the metamorphic core of the southernmost Andes and shortening in the Magallanes foreland fold and thrust belt, Tierra del Fuego, Chile. Tectonics 13 (4), 882–904.

Klepeis, K.A., Austin Jr., J.A., 1997. Contrasting styles of superposed deformation in the southernmost Andes. Tectonics 16 (5), 755–776.

Klepeis, K., Betka, P., Clarke, G., Fanning, M., Hervé, F., Rojas, L., Mpodozis, C., Thomson, S., 2010. Continental underthrusting and obduction during the cretaceous closure of the Rocas Verdes rift basin, Cordillera Darwin, Patagonian Andes. Tectonics 29 (3).

Kley, J., Monaldi, C., Salfity, J., 1999. Along-strike segmentation of the Andean foreland: causes and consequences. Tectonophysics 301 (1–2), 75–94.

König, M., Jokat, W., 2006. The Mesozoic breakup of the Weddell Sea. J. Geophys. Res. Solid Earth 111 (B12).

Koymans, M.R., Langereis, C.G., Pastor-Galán, D., van Hinsbergen, D.J., 2016. Paleomagnetism. org: An online multi-platform open source environment for paleomagnetic data analysis. Computers & Geosciences 93, 127–137.

Koymans, M., van Hinsbergen, D., Pastor-Galan, D., Vaes, B., Langereis, C., 2020. Towards FAIR paleomagnetic data management through Paleomagnetism. org 2.0. Geochem. Geophys. Geosyst. 21 (2) (e2019GC008838).

Kraemer, P.E., 1998. Structure of the Patagonian Andes: Regional balanced cross section at 50 S, Argentina. Int. Geol. Rev. 40 (10), 896–915.

Kraemer, P.E., 2003. Orogenic shortening and the origin of the Patagonian orocline (56 S. Lat). J. S. Am. Earth Sci. 15 (7), 731–748.

Kump, L.R., Brantley, S.L., Arthur, M.A., 2000. Chemical weathering, atmospheric CO2, amd climate. Annu. Rev. Earth Planet. Sci. 28, 611–667.

LaBrecque, J.L., Barker, P., 1981. The age of the Weddell basin. Nature 290 (5806), 489–492.

Lagabrielle, Y., Godderis, Y., Donnadieu, Y., Malavieille, J., Suarez, M., 2009. The tectonic history of Drake Passage and its possible impacts on global climate. Earth Planet. Sci. Lett. 279 (3–4), 197–211.

Lallemand, S., Heuret, A., Boutelier, D., 2005. On the relationships between slab dip, back-arc stress, upper plate absolute motion, and crustal nature in subduction zones. Geochem. Geophys. Geosyst. 6 (9).

Lallemand, S., Heuret, A., Faccenna, C., Funiciello, F., 2008. Subduction dynamics as revealed by trench migration. Tectonics 27 (Tc3014).

Larter, R.D., Vanneste, L.E., Morris, P., Smythe, D.K., 2003. Structure and tectonic evolution of the South Sandwich arc. Geol. Soc. Lond., Spec. Publ. 219 (1), 255–284.

LeMasurier, W.E., 2008. Neogene extension and basin deepening in the West Antarctic rift inferred from comparisons with the East African rift and other analogs. Geology 36 (3), 247–250.

Li, S., Advokaat, E.L., van Hinsbergen, D.J., Koymans, M., Deng, C., Zhu, R., 2017. Paleomagnetic constraints on the Mesozoic-Cenozoic paleolatitudinal and rotational history of Indochina and South China: Review and updated kinematic reconstruction. Earth Sci. Rev. 171, 58–77.

Lippert, P.C., Van Hinsbergen, D.J., Dupont-Nivet, G., 2014. Early cretaceous to present latitude of the central proto-Tibetan Plateau: a paleomagnetic synthesis with implications for Cenozoic tectonics, paleogeography, and climate of Asia. Geol. Soc. Am. Spec. Pap. 507, 1–21.

Livermore, R., Woollett, R., 1993. Seafloor spreading in the Weddell Sea and Southwest Atlantic since the late cretaceous. Earth Planet. Sci. Lett. 117 (3–4), 475–495.

Livermore, R., Nankivell, A., Eagles, G., Morris, P., 2005. Paleogene opening of Drake passage. Earth Planet. Sci. Lett. 236 (1–2), 459–470.

Livermore, R., Hillenbrand, C.D., Meredith, M., Eagles, G., 2007. Drake Passage and Cenozoic climate: an open and shut case? Geochem. Geophys. Geosyst. 8 (1).

Lodolo, E., Menichetti, M., Bartole, R., Ben-Avraham, Z., Tassone, A., Lippai, H., 2003. Magallanes-Fagnano continental transform fault (Tierra del Fuego, southernmost South America). Tectonics 22 (6).

Lodolo, E., Donda, F., Tassone, A., 2006. Western Scotia Sea margins: improved constraints on the opening of the Drake Passage. J. Geophys. Res. Solid Earth 111 (B6).

Lodolo, E., Civile, D., Vuan, A., Tassone, A., Geletti, R., 2010. The Scotia–Antarctica plate boundary from 35 W to 45 W. Earth Planet. Sci. Lett. 293 (1–2), 200–215.

Longshaw, S., Griffiths, D., 1983. A palaeomagnetic study of Jurassic rocks from the Antarctic Peninsula and its implications. J. Geol. Soc. 140 (6), 945–954.

Luyendyk, B.P., Sorlien, C.C., Wilson, D.S., Bartek, L.R., Siddoway, C.S., 2001. Structural and tectonic evolution of the Ross Sea rift in the Cape Colbeck region, Eastern Ross Sea, Antarctica. Tectonics 20 (6), 933–958.

Macdonald, D., Gomez-Perez, I., Franzese, J., Spalletti, L., Lawver, L., Gahagan, L., Dalziel, I., Thomas, C., Trewin, N., Hole, M., 2003. Mesozoic break-up of SW Gondwana: implications for regional hydrocarbon potential of the southern South Atlantic. Mar. Pet. Geol. 20 (3–4), 287–308.

Maffione, M., 2016. Kinematic evolution of the Southern Andean orogenic arc. In: Geodynamic Evolution of the Southernmost Andes. Springer, pp. 173–200.

Maffione, M., Speranza, F., Faccenna, C., Rossello, E., 2010. Paleomagnetic evidence for a pre-early Eocene (~ 50 Ma) bending of the Patagonian orocline (Tierra del Fuego, Argentina): Paleogeographic and tectonic implications. Earth Planet. Sci. Lett. 289 (1–2), 273–286.

Maffione, M., Thieulot, C., Van Hinsbergen, D.J., Morris, A., Plümper, O., Spakman, W., 2015. Dynamics of intraoceanic subduction initiation: 1. Oceanic detachment fault inversion and the formation of supra-subduction zone ophiolites. Geochem. Geophys. Geosyst. 16 (6), 1753–1770.

Maloney, K., Clarke, G., Klepeis, K., Fanning, C., Wang, W., 2011. Crustal growth during back-arc closure: cretaceous exhumation history of Cordillera Darwin, southern Patagonia. J. Metamorph. Geol. 29 (6), 649–672.

Mao, S., Mohr, B., 1995. Middle Eocene dinocysts from Bruce Bank (Scotia Sea, Antarctica) and their paleoenvironmental and paleogeographic implications. Rev. Palaeobot. Palynol. 86 (3–4), 235–263.

Marshak, S., 1988. Kinematics of orocline and arc formation in thin-skinned orogens. Tectonics 7 (1), 73–86.

Matthews, D.H., Maling, D.H., 1967. The geology of the South Orkney Islands: I. Signy Island. FIDS Scientific Reports 25, 1–32.

McAtamney, J., Klepeis, K., Mehrtens, C., Thomson, S., Betka, P., Rojas, L., Snyder, S., 2011. Along-strike variability of back-arc basin collapse and the initiation of sedimentation in the Magallanes foreland basin, southernmost Andes (53–54.5° S). Tectonics 30 (5).

Meert, J.G., Pivarunas, A.F., Evans, D.A., Pisarevsky, S.A., Pesonen, L.J., Li, Z.-X., Elming, S.-Å., Miller, S.R., Zhang, S., Salminen, J.M., 2020. The magnificent seven: a proposal for modest revision of the quality index. Tectonophysics 228549.

Milanese, F.N., Olivero, E.B., Kirschvink, J.L., Rapalini, A.E., 2017. Magnetostratigraphy of the Rabot formation, upper cretaceous, James Ross Basin, antarctic Peninsula. Cretac. Res. 72, 172–187.

Milanese, F., Rapalini, A., Slotznick, S.P., Tobin, T.S., Kirschvink, J., Olivero, E., 2019. Late cretaceous paleogeography of the Antarctic Peninsula: New paleomagnetic pole from the James Ross Basin. J. S. Am. Earth Sci. 91, 131–143.

Moulin, M., Aslanian, D., Unternehr, P., 2010. A new starting point for the South and Equatorial Atlantic Ocean. Earth Sci. Rev. 98 (1–2), 1–37.

Mueller, C.O., Jokat, W., 2019. The initial Gondwana break-up: a synthesis based on new potential field data of the Africa-Antarctica Corridor. Tectonophysics 750, 301–328.

Mukasa, S.B., Dalziel, I.W., 1996. Southernmost Andes and South Georgia Island, North Scotia Ridge: zircon U-Pb and muscovite 40Ar39Ar age constraints on tectonic evolution of Southwestern Gondwanaland. J. S. Am. Earth Sci. 9 (5–6), 349–365.

Müller, R., Gohl, K., Cande, S., Goncharov, A., Golynsky, A., 2007. Eocene to Miocene geometry of the West Antarctic rift system. Aust. J. Earth Sci. 54 (8), 1033–1045.

Müller, R.D., Seton, M., Zahirovic, S., Williams, S.E., Matthews, K.J., Wright, N.M., Shephard, G.E., Maloney, K.T., Barnett-Moore, N., Hosseinpour, M., 2016. Ocean

basin evolution and global-scale plate reorganization events since Pangea breakup. Annu. Rev. Earth Planet. Sci. 44, 107–138.

Müller, R.D., Zahirovic, S., Williams, S.E., Cannon, J., Seton, M., Bower, D.J., Tetley, M. G., Heine, C., Le Breton, E., Liu, S., 2019. A global plate model including lithospheric deformation along major rifts and orogens since the Triassic. Tectonics 38 (6), 1884–1907.

Navarrete, C., Gianni, G., Encinas, A., Márquez, M., Kamerbeek, Y., Valle, M., Folguera, A., 2019. Triassic to Middle Jurassic geodynamic evolution of southwestern Gondwana: from a large flat-slab to mantle plume suction in a rollback subduction setting. Earth Sci. Rev. 194, 125–159.

Nerlich, R., Clark, S.R., Bunge, H.-P., 2013. The Scotia Sea gateway: no outlet for Pacific mantle. Tectonophysics 604, 41–50.

Olivero, E.B., Malumián, N., 2008. Mesozoic-Cenozoic stratigraphy of the Fuegian Andes, Argentina. Geol. Acta 6 (1), 5–18.

Owen-Smith, T.M., Ganerød, M., van Hinsbergen, D.J., Gaina, C., Ashwal, L.D., Torsvik, T.H., 2019. Testing early cretaceous Africa–South America fits with new palaeomagnetic data from the Etendeka Magmatic Province (Namibia). Tectonophysics 760, 23–35.

Pandey, A., Parson, L., Milton, A., 2010. Geochemistry of the Davis and Aurora banks: possible implications on evolution of the North Scotia Ridge. Mar. Geol. 268 (1–4), 106–114.

Pankhurst, R., Riley, T., Fanning, C., Kelley, S., 2000. Episodic silicic volcanism in Patagonia and the Antarctic Peninsula: chronology of magmatism associated with the break-up of Gondwana. J. Petrol. 41 (5), 605–625.

Pearce, J., Hastie, A., Leat, P., Dalziel, I., Lawver, L., Barker, P., Millar, I., Barry, T., Bevins, R., 2014. Composition and evolution of the Ancestral South Sandwich Arc: Implications for the flow of deep ocean water and mantle through the Drake Passage Gateway. Glob. Planet. Chang. 123, 298–322.

Pelayo, A.M., Wiens, D.A., 1989. Seismotectonics and relative plate motions in the Scotia Sea region. J. Geophys. Res. Solid Earth 94 (B6), 7293–7320.

Pérez-Díaz, L., Eagles, G., 2014. Constraining South Atlantic growth with seafloor spreading data. Tectonics 33 (9), 1848–1873.

Poblete, F., Arriagada, C., Roperch, P., Astudillo, N., Hervé, F., Kraus, S., Le Roux, J., 2011. Paleomagnetism and tectonics of the South Shetland Islands and the northern Antarctic Peninsula. Earth Planet. Sci. Lett. 302 (3–4), 299–313.

Poblete, F., Roperch, P., Arriagada, C., Ruffet, G., de Arellano, C.R., Hervé, F., Poujol, M., 2016. Late Cretaceous–early Eocene counter-clockwise rotation of the Fuegian Andes and evolution of the Patagonia–Antarctic Peninsula system. Tectonophysics 668, 15–34.

Rapalini, A.E., Tohver, E., Bettucci, L.S., Lossada, A.C., Barcelona, H., Pérez, C., 2015. The late Neoproterozoic Sierra de las Ánimas Magmatic complex and Playa Hermosa Formation, southern Uruguay, revisited: Paleogeographic implications of new paleomagnetic and precise geochronologic data. Precambrian Res. 259, 143–155.

Rapela, C., Pankhurst, R., 1992. The granites of northern Patagonia and the Gastre Fault System in relation to the break-up of Gondwana. Geol. Soc. Lond., Spec. Publ. 68 (1), 209–220.

Riley, T.R., Knight, K.B., 2001. Age of pre-break-up Gondwana magmatism. Antarct. Sci. 13 (2), 99–110.

Riley, T.R., Carter, A., Leat, P.T., Burton-Johnson, A., Bastias, J., Spikings, R.A., Tate, A. J., Bristow, C.S., 2019. Geochronology and geochemistry of the northern Scotia Sea: a revised interpretation of the North and West Scotia ridge junction. Earth Planet. Sci. Lett. 518, 136–147.

Royer, J.Y., Chang, T., 1991. Evidence for relative motions between the Indian and Australian plates during the last 20 my from plate tectonic reconstructions: Implications for the deformation of the Indo-Australian plate. J. Geophys. Res. Solid Earth 96 (B7), 11779–11802.

Salabarnada, A., Escutia, C., Röhl, U., Nelson, C.H., McKay, R., Jiménez-Espejo, F., Bijl, P., Hartman, J., Strother, S., Salzmann, U., 2018. Paleoceanography and ice sheet variability offshore Wilkes Land, Antarctica–Part 1: Insights from late Oligocene astronomically paced contourite sedimentation. Clim. Past 14 (7), 991–1014.

Sangiorgi, F., Bijl, P.K., Passchier, S., Salzmann, U., Schouten, S., McKay, R., Cody, R.D., Pross, J., Van De Flierdt, T., Bohaty, S.M., 2018. Southern Ocean warming and Wilkes Land ice sheet retreat during the mid-Miocene. Nat. Commun. 9 (1), 1–11.

Schellart, W.P., 2005. Influence of the subducting plate velocity on the geometry of the slab and migration of the subduction hinge. Earth Planet. Sci. Lett. 231 (3–4), 197–219.

Schellart, W.P., 2017. Andean mountain building and magmatic arc migration driven by subduction-induced whole mantle flow. Nat. Commun. 8, 2010.

Schepers, G., Van Hinsbergen, D.J., Spakman, W., Kosters, M.E., Boschman, L.M., McQuarrie, N., 2017. South-American plate advance and forced Andean trench retreat as drivers for transient flat subduction episodes. Nat. Commun. 8, 15249.

Scher, H.D., Martin, E.E., 2006. Timing and climatic consequences of the opening of Drake Passage. Science 312 (5772), 428–430.

Schimschal, C.M., Jokat, W., 2018. The crustal structure of the continental margin east of the Falkland Islands. Tectonophysics 724, 234–253.

Schimschal, C.M., Jokat, W., 2019. The Falkland Plateau in the context of Gondwana breakup. Gondwana Res. 68, 108–115.

Schreider, A.A., Schreider, A., Galindo-Zaldívar, J., Maldonado, A., Sazhneva, A., Evsenko, E., 2017. Age of the scan basin (Scotia Sea). Oceanology 57 (2), 328–336.

Schreider, A.A., Schreider, A., Galindo-Zaldívar, J., Maldonado, A., Sazhneva, A., Evsenko, E., 2018. Age of the floors of the protector and dove basins (Scotia Sea). Oceanology 58 (3), 447–458.

Scott, K.M., 1966. Sedimentology and dispersal pattern of a cretaceous flysch sequence, Patagonian Andes, southern Chile. AAPG Bull. 50 (1), 72–107.

Sijp, W.P., Anna, S., Dijkstra, H.A., Flögel, S., Douglas, P.M., Bijl, P.K., 2014. The role of ocean gateways on cooling climate on long time scales. Glob. Planet. Chang. 119, 1–22.

Smalley Jr., R., Kendrick, E., Bevis, M., Dalziel, I., Taylor, F., Lauría, E., Barriga, R., Casassa, G., Olivero, E., Piana, E., 2003. Geodetic determination of relative plate motion and crustal deformation across the Scotia-South America plate boundary in eastern Tierra del Fuego. Geochem. Geophys. Geosyst. 4 (9).

Smalley Jr., R., Dalziel, I., Bevis, M., Kendrick, E., Stamps, D., King, E., Taylor, F., Lauría, E., Zakrajsek, A., Parra, H., 2007. Scotia arc kinematics from GPS geodesy. Geophys. Res. Lett. 34 (21).

Smalley Jr., R., Dalziel, I.W., Lawver, L.A., Gómez, D., Teferle, F.N., Saustrup, S., Hunegnaw, A., 2019. The current tectonic setting of South Georgia Island based on GPS geodetic and marine seismic reflection data. AGUFM 2019, G34A–01.

Spakman, W., Hall, R., 2010. Surface deformation and slab–mantle interaction during Banda arc subduction rollback. Nat. Geosci. 3 (8), 562–566.

Spakman, W., Chertova, M.V., van den Berg, A., van Hinsbergen, D.J., 2018. Puzzling features of western Mediterranean tectonics explained by slab dragging. Nat. Geosci. 11 (3), 211–216.

Stern, C.R., Mukasa, S.B., Fuenzalida, R.H., 1992. Age and petrogenesis of the Sarmienot ophiolite complex of southern Chile. Journal of South American Earth Sciences 6 (1–2), 97–104.

Stern, R.J., 2004. Subduction initiation: spontaneous and induced. Earth Planet. Sci. Lett. 226 (3–4), 275–292.

Stern, C.R., De Wit, M.J., 2003. Rocas Verdes ophiolites, southernmost South America: Remnants of progressive stages of development of oceanic-type crust in a continental margin back-arc basin. Geol. Soc. Lond., Spec. Publ. 218 (1), 665–683.

Storey, B., Mair, B., 1982. The composite floor of the cretaceous back-arc basin of South Georgia. J. Geol. Soc. 139 (6), 729–737.

Storey, B., Mair, B., Bell, C., 1977. The occurrence of Mesozoic oceanic floor and ancient continental crust on South Georgia. Geol. Mag. 114 (3), 203–208.

Storey, B.C., Vaughan, A.P., Millar, I.L., 1996. Geodynamic evolution of the Antarctic Peninsula during Mesozoic times and its bearing on Weddell Sea history. Geol. Soc. Lond., Spec. Publ. 108 (1), 87–103.

Suárez, M., 1976. Plate-tectonic model for southern Antarctic Peninsula and its relation to southern Andes. Geology 4 (4), 211–214.

Tankard, A.J., Martin, M., Eriksson, K., Hobday, D., Hunter, D., Minter, W., 2012. Crustal Evolution of Southern Africa: 3.8 Billion Years of Earth History. Springer Science & Business Media.

Tanner, P., Pankhurst, R., Hyden, G., 1982. Radiometric evidence for the age of the subduction complex in the South Orkney and South Shetland Islands, West Antarctica. J. Geol. Soc. 139 (6), 683–690.

Tauxe, L., Kent, D.V., 2004. A Simplified Statistical Model for the Geomagnetic Field and the Detection of Shallow Bias in Paleomagnetic Inclinations: Was the Ancient Magnetic Field Dipolar?.

Thomas, C., Livermore, R., Pollitz, F., 2003. Motion of the Scotia Sea plates. Geophys. J. Int. 155, 789–804.

Tingey, R.J., 1991. The Geology of Antarctica. Oxford University Press.

Torres-Carbonell, P.J., Dimieri, L.V., 2013. Cenozoic contractional tectonics in the Fuegian Andes, southernmost South America: a model for the transference of orogenic shortening to the foreland. Geol. Acta 11 (3), 331–357.

Torres-Carbonell, P.J., Olivero, E.B., 2012. Sand dispersal in the southeastern Austral Basin, Tierra del Fuego, Argentina: Outcrop insights from Eocene channeled turbidite systems. J. S. Am. Earth Sci. 33 (1), 80–101.

Torres-Carbonell, P.J., Olivero, E.B., Dimieri, L.V., 2008a. Control en la magnitud de desplazamiento de rumbo del Sistema Transformante Fagnano, Tierra del Fuego, Argentina. Rev. Geol. Chile 35 (1), 63–77.

Torres-Carbonell, P.J., Olivero, E.B., Dimieri, L.V., 2008b. Structure and evolution of the Fuegian Andes foreland thrust-fold belt, Tierra del Fuego, Argentina: Paleogeographic implications. J. S. Am. Earth Sci. 25 (4), 417–439.

Torres-Carbonell, P.J., Dimieri, L.V., Olivero, E.B., 2011. Progressive deformation of a Coulomb thrust wedge: the eastern Fuegian Andes thrust-fold belt. Geol. Soc. Lond., Spec. Publ. 349 (1), 123–147.

Torres-Carbonell, P.J., Dimieri, L.V., Martinioni, D.R., 2013. Early foreland deformation of the Fuegian Andes (Argentina): Constraints from the strain analysis of Upper Cretaceous-Danian sedimentary rocks. J. Struct. Geol. 48, 14–32.

Torres-Carbonell, P.J., Dimieri, L.V., Olivero, E.B., Bohoyo, F., Galindo-Zaldívar, J., 2014. Structure and tectonic evolution of the Fuegian Andes (southernmost South America) in the framework of the Scotia Arc development. Glob. Planet. Chang. 123, 174–188.

Torres-Carbonell, P.J., Rodríguez Arias, L., Atencio, M.R., 2017. Geometry and kinematics of the Fuegian thrust-fold belt, southernmost Andes. Tectonics 36 (1), 33–50.

Torsvik, T.H., Müller, R.D., Van der Voo, R., Steinberger, B., Gaina, C., 2008. Global plate motion frames: toward a unified model. Rev. Geophys. 46 (3).

Torsvik, T.H., Rousse, S., Labails, C., Smethurst, M.A., 2009. A new scheme for the opening of the South Atlantic Ocean and the dissection of an Aptian salt basin. Geophys. J. Int. 177 (3), 1315–1333.

Torsvik, T.H., Van der Voo, R., Preeden, U., Mac Niocaill, C., Steinberger, B., Doubrovine, P.V., Van Hinsbergen, D.J., Domeier, M., Gaina, C., Tohver, E., 2012. Phanerozoic polar wander, palaeogeography and dynamics. Earth Sci. Rev. 114 (3–4), 325–368.

Torsvik, T.H., Doubrovine, P.V., Steinberger, B., Gaina, C., Spakman, W., Domeier, M., 2017. Pacific plate motion change caused the Hawaiian-Emperor Bend. Nat. Commun. 8 (1), 1–12.

Udintsev, G., Kurentsova, N., Beresnev, A., Kol'tsova, A., Domoratskaya, L., Schenke, G., Bakhmutov, V., Solov'ev, V., 2012. Tectonics of the Drake Passage-Scotia Sea Zone in the Southern Ocean, Doklady Earth Sciences. Springer, pp. 1029–1035.

Vaes, B., Van Hinsbergen, D.J., Boschman, L.M., 2019. Reconstruction of subduction and back-arc spreading in the NW Pacific and Aleutian Basin: Clues to causes of Cretaceous and Eocene plate reorganizations. Tectonics 38 (4), 1367–1413.

Vaes, B., Li, S., Langereis, C.G., van Hinsbergen, D.J.J., 2021. Reliability criteria for paleomagnetic poles from clastic sedimentary rocks. Geophys. J. Int. https://doi.org/10.1093/gji/ggab016.

van de Lagemaat, S.H., van Hinsbergen, D.J., Boschman, L.M., Kamp, P.J., Spakman, W., 2018. Southwest Pacific absolute plate kinematic reconstruction reveals major Cenozoic Tonga-Kermadec slab dragging. Tectonics 37 (8), 2647–2674.

Van der Meer, D.G., Van Hinsbergen, D.J., Spakman, W., 2018. Atlas of the underworld: Slab remnants in the mantle, their sinking history, and a new outlook on lower mantle viscosity. Tectonophysics 723, 309–448.

van Hinsbergen, D.J.J., Schouten, T.L.A., 2021. Deciphering paleogeography from orogenic architecture: constructing orogens in a future supercontinent as thought experiment. Am. J. Sci. https://doi.org/10.31223/X5M895. Eartharxiv (in press).

Van Hinsbergen, D.J.J., Hafkenscheid, E., Spakman, W., Meulenkamp, J., Wortel, R., 2005. Nappe stacking resulting from subduction of oceanic and continental lithosphere below Greece. Geology 33 (4), 325–328.

van Hinsbergen, D.J., Peters, K., Maffione, M., Spakman, W., Guilmette, C., Thieulot, C., Plümper, O., Gürer, D., Brouwer, F.M., Aldanmaz, E., 2015. Dynamics of intraoceanic subduction initiation: 2. Suprasubduction zone ophiolite formation and metamorphic sole exhumation in context of absolute plate motions. Geochem. Geophys. Geosyst. 16 (6), 1771–1785.

Van Hinsbergen, D.J., Torsvik, T.H., Schmid, S.M., Maţenco, L.C., Maffione, M., Vissers, R.L., Gürer, D., Spakman, W., 2020. Orogenic architecture of the Mediterranean region and kinematic reconstruction of its tectonic evolution since the Triassic. Gondwana Res. 81, 79–229.

Vanneste, L.E., Larter, R.D., 2002. Sediment subduction, subduction erosion, and strain regime in the northern South Sandwich forearc. J. Geophys. Res. Solid Earth 107 (B7) (EPM 5-1-EPM 5–24).

Vérard, C., Flores, K., Stampfli, G., 2012. Geodynamic reconstructions of the South America–Antarctica plate system. J. Geodyn. 53, 43–60.

Von Gosen, W., Loske, W., 2004. Tectonic history of the Calcatapul Formation, Chubut province, Argentina, and the "Gastre fault system". J. S. Am. Earth Sci. 18 (1), 73–88.

Vuan, A., Lodolo, E., Panza, G., Sauli, C., 2005. Crustal structure beneath Discovery Bank in the Scotia Sea from group velocity tomography and seismic reflection data. Antarct. Sci. 17 (1), 97–106.

Watts, D.R., Watts, G.C., Bramall, A., 1984. Cretaceous and early Tertiary paleomagnetic results from the Antarctic Peninsula. Tectonics 3 (3), 333–346.

Whittaker, J.M., Müller, R.D., Leitchenkov, G., Stagg, H., Sdrolias, M., Gaina, C., Goncharov, A., 2007. Major Australian-Antarctic Plate Reorganization at Hawaiian-Emperor Bend Time. Science 318, 83–86.

Willan, R.C., Hunter, M.A., 2005. Basin evolution during the transition from continental rifting to subduction: evidence from the lithofacies and modal petrology of the Jurassic Latady Group, Antarctic Peninsula. J. S. Am. Earth Sci. 20 (3), 171–191.

Wilson, T.J., 1991. Transition from back-arc to foreland basin development in the southernmost Andes: Stratigraphic record from the Ultima Esperanza District, Chile. Geol. Soc. Am. Bull. 103 (1), 98–111.

Winn Jr., R., 1978. Upper Mesozoic flysch of Tierra del Fuego and South Georgia Island: a sedimentologic approach to lithosphere plate restoration. Geol. Soc. Am. Bull. 89 (4), 533–547.

Zaffarana, C., Somoza, R., Mercader, R., Giacosa, R., Martino, R., 2010. Anisotropy of magnetic susceptibility study in two classical localities of the Gastre Fault System, Central Patagonia. J. S. Am. Earth Sci. 30 (3–4), 151–166.

Zaffarana, C.B., Somoza, R., Orts, D.L., Mercader, R., Boltshauser, B., González, V.R., Puigdomenech, C., 2017. Internal structure of the late Triassic Central Patagonian batholith at Gastre, southern Argentina: Implications for pluton emplacement and the Gastre fault system. Geosphere 13 (6), 1973–1992.